CR 151592

FINAL REPORT ON DESIGN & FABRICATION OF NOSECONE FOR WB-57F AIRCRAFT

Hacking Labs, Santa Clara, CA. 95050

(NASA-CR-151592) DESIGN AND FABRICATION OF NOSECONE FOR WB-57F AIRCRAFT FITTED WITH APQ-102A SIDE LOOKING RADAR Final Report (Hacking Labs., Santa Clara, Calif.) 104 p HC A06/MF A01

N78-15028

CSCL 01C G3/05

Unclas 57759

FINAL REPORT

ON

DESIGN & FABRICATION

OF

NOSECONE FOR WB-57F AIRCRAFT

FITTED WITH

APQ-102A SIDE LOOKING RADAR

Prepared for

Lyndon B. Johnson Space Center

NASA

Houston TX 77058

Prepared by

HACKING LABS, SANTA CLARA, CA

Contract No. NAS 9-15189

HL Project No. 22

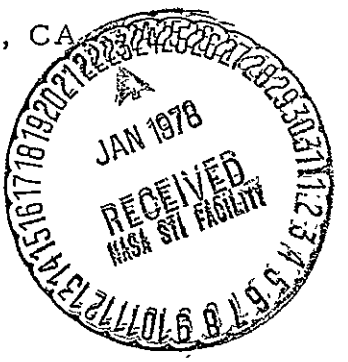

December 1977

TABLE OF CONTENTS (contd.)

TABLE OF CONTENTS

1. SCOPE

The contract work consisted of the design, fabrication, and testing of a nosecone which included a radome for a NASA WB-57F high altitude natural resources mapping aircraft. The plane was fitted with a Motorola APQ-102A Side Looking Radar operating at 9.6 GHz. The radar is directed normal to the direction of the flight and downward by a changeable angle, and it is assumed that the axis of the plane will not deviate from this direction by more than $\pm 6^{o}$. The radome is required to subtend an angle of 160^{o} centered 30^{o} below the left horizon. The nosecone shape would be the same as one supplied by NASA for a similar plane, except that it would be a complete surface of revolution without protrusions for photographic equipment. Its size would be 75.5" long and 48" in diameter at its attach end. Operational altitude was up to 60,000 feet and a speed up to 400 knots. The various components of the work are reported in this final report, but not necessarily in the order of performance.

2. TECHNICAL CONTENT

The project consisted of the following separate parts, some of which were performed in parallel.

a) Aerodynamic Analysis

b) Microwave Design

c) Structural Conception

d) Structural Analysis

e) Fabrication Technique Design

f) Sample Fabrications

g) RF and Mechanical Tests on Samples

h) Mold Design and Fabrication

i) Radome Fabrication

j) Foam Machining Tools and Fabrication

k) RF Test Tool Design and Fabrication

l) RF Testing of Radome

m) Back Portion Fabrication

n) Design and Fabrication

o) Integration of Two Halves

p) Fabrication of Interface with Aircraft

q) High Temperature Post Cure

r) Installation of Auxilliary Equipment (GFE)

s) Pressure Test

t) Surface Clean-up and Sealing

u) Crating and Shipping

v) Monthly Reports, Final Report and Drawings

3. BASIC DESIGN CONCEPTS

This discussion concerns both RF and mechanical aspects. Several cross sectional configurations of radome were considered. These are shown in Fig. 1. and are discussed briefly below:

3.1 Quarterwave "A" Sandwich. This consits of 2 structural skins, ideally having equal RF susceptances, separated by means of low dielectric constant material such that the two primary susceptances cancel each other over most of the operating conditions. This spacing is usually approximately .2 wavelengths, although it is commonly categorized as one quarter wavelength. It is the lightest possible radome structure in which any attempt is made to effect an RF match. It has high resistance to bending per unit weight. It does have the complication of being made of three component parts. It will be treated as the reference against which the other configuration will be compared.

3.2 The Three-quarter Wavelength Sandwich. This device is similar to 3.1 above except that the low dielectric material has a thickness of approximately .7 wavelengths. This greatly increases the resistance to bending, has little effect on the weight, but greatly reduces the effective bandwidth of the radome to about 1/3 that of the quarter-wave sandwich. It is often appropriate for use at mm waves. (Note that effective bandwidth takes into account both actual frequency bandwidth and the effect of a range of incidence angles.)

3.3 The C-Type Sandwich. This consists of 3 layers of high dielectric (and presumably high strength) material and 2 sections of low dielectric material. It can be considered as 2 "A"-Type structures up against each other. Since the mean spacing between two such structures is approximately quarter wavelength, any reflection from one structure will be cancelled out by the equal and opposite reflection from the other. This "C"-Type radome, therefore, has a good match over a much wider effective bandwidth than the simple quarterwave sandwich. It is of course also more complex and has its strongest element, which is generally 1.5 to 2 times as thick as the outer skins, buried within the structure where it contributes nothing to the bending strength and could cause a heat dissipation problem under high power condition, because of the insulation qualities of the low dielectric constant material.

3.4 Half-wavelength Solid Radome. This is the simplest of the four structures considered, but also the heaviest and most lossy. It has about the same overall thickness as the A-Type radome and about half its effective bandwidth. It is appreciably stronger with much higher heat transfer properties.

4. CHOICE OF RADOME STRUCTURE

Due to the symmetry of the nosecone, high resistance to bending is not especially important so that the solid half-wavelength

and three-quarter sandwich configuration offer no appreciable advantages and some considerable disadvantages. Although the frequency of operation is fixed in the present application, the effective bandwidth is approximately 30% due to the wide range of angles of incidence of the radar antenna near-field radiation with the radome. These angles have somewhat arbitrarily been considered to range from $2 < \theta < 40^{o}$. The effective wavelength is given by secant θ times the real wavelength, which is $\frac{11.8}{9.6} = 1.23$ in. Thus the effective wavelength varies between 1.23 and 1.60 giving a nominal mean quarter-wavelength of .35 inches.

4.1 Considerations of C-Type Radome. This configuration was seriously considered for this application, since it would greatly reduce reflections at high incidence angles. However, after discussion with personnel at Goodyear Co. in Pheonix, builders of the APQ-102A radar, it became apparent that this configuration represented an unnecessary complication, since such reflections were not considered to be a problem. In addition if the same outer envelope were used the inside volume would be decreased to a point where there was a much higher risk of interference with the radar when in its extreme positions. This configuration would also have higher absorption loss (attenuation) and would offer no significant mechanical advantages. It was therefore decided not to pursue this configuration and to concentrate on the "A" type quarterwave sandwich.

5. EXPERIMENTAL INVESTIGATION

Experience has shown that for an A sandwich radome a core thickness of somewhat less than .2 wavelengths is generally the optimum value. At the higher frequencies this is somewhat dependent on the exact method of fabrication, and consequent distribution of resin within the structure.

Several samples of flat radome panels were made, using the same fabrication technique that would be used for the final radome. From this work and subsequent RF measurements, it was determined that thickness of .250 inches was most suitable for the particular 4 lb/C.F. foam core to be used, considering angles of incidence of up to 40^{o}.

RF transmission measurements were made on these flat samples using the measurement set-up shown in Fig.2. Provision was made to move the whole rotating pedestal by a quarter wavelength (.32 in.) so as to average out the effects of mismatches of the various components and other undesired radiation from the environment.

5.1 Typical Results. Some samples of transmission recorded as a function of angle of incidence for two of the samples are shown in Figs. 3. through 6. Each measurement was made twice to indicate the repeatability of the measurements. This repeatability was only approximately .05dB, but other variations were much larger. No attempt is made to explain the exact reasons for all the characteristics of these

recordings, except to note that the average transmission loss is typically .2dB or less when the correct core thickness is used, and it starts to increase at angles of $\pm 40^{o}$, especially where the E field is perpendicular to the angle of incidence (parallel to the axis of rotation. The Brewster angle effect reduces this effect in the orthogenal polarization case.) It can also be seen that there is apparentl- an .8dB attenuation in Fig. 6 at plus 50^{o}. This data is not to be taken at face value, since RF energy is no doubt being scattered by the edge of the sample. Also the region of the particular sample geing illuminated consisted of solid fiberglass rather than foam sandwich. The example is useful in showing that spurious data will be obtained near the edge of any device being measured. This effect becomes much more apparent in the final RF tests on the finished radome.

6. PRIMARY MOLD

6.1 Preparation of Old Nosecone. The old nosecone (GFE) was prepared for use for a mold to make the molds from which the final radome and nosecone would be fabricated. It was discovered that this old nosecone did not fit the dimensions supplied in the RFP in that the spherical portion in the front of the nosecone had a somewhat larger radius than 15 inches and the conical portion was not truly conical. The nominal angle of the cone is somewhat smaller than the figure shown on the sketches provided with the RFP.

Because of the very rough surface of the existing nosecone and the irregularities on it, considerably more time was taken in preparing this nosecone as a mold than had been anticipated. In retrospect, we now believe that it probably would have been more expeditious to start from scratch and make an entirely new mold. The discrepancies in the dimensions of the nosecone were only determined after the process of laying out coordinate lines on the the existing nosecone. Due to the assymmetry of the nosecone, optical tooling techniques had to be used for making these layouts.

Further irregularities of this nosecone became apparent when the two new nosecone halves had to be joined together.

6.2 Mold Fabrications. Since the GFE nosecone is not completely circularly symmetric, only its upper portion could be used as a mold. It was used to make the primary mold which was exactly one half plus 6 inches all the way around. This mold was made of polyester resin with a black gelcoat surface and rolled steel pipe and other steel reinforcing to help maintain shape. When set on the ground (on its built-in steel legs) in a horizontal axis position this mold was convenient to work in for laying up the nosecone components.

7. GENERAL FABRICATION CONSIDERATIONS

The decision to use fiberglass foam sandwich was made based on previous experience in fabricating radomes using this combination of materials rather than the more common honeycomb core.

The primary differences between foam and honeycomb are that the honeycomb is slightly stronger, especially in shear for the same density, than the foam, but does not present as much area for bonding to the skins. The foam, of course, bonds over its full area, provided an adequate pressure of a few psi is applied during resin curing. Very often closed mold autoclave techniques are the only ones feasible for fabricating honeycomb radomes, and this is a very expensive procedure, especially so when only one unit is required, becuase of the tooling costs.

Our procedure makes use of almost full atmospheric pressure (approximately 13 psi) for a very good bond between the fiberglass and the core material. So called "vacuum bagging" is well known in the fiberglass industry, but the technique which we used is quite different from the usual procedure in which each layer (fiberglass, foam, fiberglass) would be bagged separately. It is common practice to lay up and cure the outer skin in the mold as a first step, using a vacuum bag which serves the dual purpose of sqeezing all the fibers together into the thinest possible laminate and also drawing off the excess resin which is later discarded. The next step is to do the same thing with the foam core, but this requires a suitable additional bond material to bond the foam to the cured outer skin. This bonding material, which is generally a resin-filler mixture, cannot be made negligible, so it will almost certainly deteriorate the RF match of the radome. It is not feasible to draw off the excess resin in this operation, as is possible with the

solid fiberglass laminates. The third bagging operation must then be performed. This involves lay-up of the inner skin which will, in general, have the same thickness as the outer skin, using exactly the same procedure as for the first skin. However, since some of the excess resin will be squeezed into the foam this skin will have a higher resin content.

In the Hacking Lab's process no special bonding agent is employed to bond the foam to either skin. The resin used for this purpose is simply the same resin as is used to laminate the respective skin. Care must be taken not to have any excess resin in either laminate since the procedure used does not permit the complete drawing off of any excess resin. It is, therefore, very important to control the weight of resin used per unit area of fiberglass. We have found by experience that the weight of resin should be approximately 35% of the weight of the wet laminate. This ratio also corresponds with the optimum content of resin to provide the best strength to weight of a fiberglass laminate using the particular fabric chosen for the laminating (Type 181).

7.1 Specific Resin and Foam System. The resin chosen for fabricating the radome (and most of the rest of the nosecone) was Shell Epon 815 epoxy resin with Furane 9111 Hardener. This is a slow, room temperature cure system which normally takes several days to reach its final strength but can be accelerated by a post-cure of 2 to 4 hours at 160°F or above.

The foam used as the core material was Upjohn Co.'s CPR 9006-4. Our first choice was the 9002 system, but this no longer appears to be manufactured.

7.2 Specific Fabrication Technique. Using this company fabrication method the whole sandwich is made in one operation. It does require two conditions which are not needed in most other methods. These are

a) The core material must be grooved in such a manner that air passages are maintained over the whole surface in order to extract air everywhere. This is necessary to ensure that atmospheric pressure can be applied in a more or less uniform manner over the complete laminate.

b) The combination of resin system and curing temperature must be such that the whole laminating process can be completed before set-up begins. This may require working odd hours of the day in order to take advantage of the low ambient temperatures, since set-up time is very dependent on temperature. The alternative, of course, is to use an air conditioned room, but this is generally undesirable, because of the need for venting the resin gases which are not very pleasant to work around and could be toxic if not dispersed.

In the present case laminating 50% of the nosecone at one time required an elapsed time of approximately 6 hours with a work force of 5 or 6 people. This time does not include

the time needed to prepare all the materials to be used.

The cloth and resin were all prepared in advance and were readily available when needed. As already indicated it is necessary to have quite accurate control of the resin to fiberglass ratio, so the weight of each piece of glass had to be known and the corresponding weight of resin prepared to be used with that piece of glass. The minimum amount of hardener was used consistent with a good strength laminate (16%), in order to delay the set-up time of the resin as long as possible. Because the exact amount of hardener had to be applied to each batch of resin for each particular piece of glass, the quantities of hardener are quite small and in order to maintain accurate control they were dispensed with a hypodermic syringe. In a further effort to extend set-up time to a maximum the resin/hardener mixture was spread onto the glass fabric as soon as it was vigorously mixed in order to permit the exothermal mixing heat to dissipate as soon as possible.

7.3 Vacuum System. To assist in the evacuation process, that is to implement the "bagging" operation, vacuum pump suction points were fitted to the mold over its entire area. These were then attached together in a vacuum manifold system. Although the foam was scored in a very systematic manner so that there were no areas with grooves more than one inch apart, it was still felt necessary to provide redundant air paths in case one or more of the grooves clog with

resin during the evacuation process. Due to the low pressures involved and the generally high viscosity of the resin, which was purposely kept as cool as possible, movement of excessive resin through a long narrow passage could cause loss of atmospheric pressure on the laminate if any air leaks or outgassing occured. Since the resin had been carefully weighed out to give the correct resin-to-glass ratio, it was assumed that there would be no excess resin to draw off, so no provision was made for drawing the resin to the plastic bagging surface as is usually done. There will always be some excess resin, but we wanted this to be drawn inward toward the foam so as to ensure a better bond to the foam rather than to draw it to the outside of the laminate to be absorbed in a material which would later be discarded. By this method we were assured of having equal quantities of resin in the front and back skins of the sandwich, whus assuring equal RF susceptances of the two skins and therefore the best possible RF match for the incident radiation.

Several suction points were fitted to the mold and connected together and to a vacuum pump during fabrication. This resulted in small holes in the finished part, which had to be repaired. This was done by fitting the holes with a mixture of resin and very light filler (microballoons). The resultant mixture has a specific gravity of approximately .5 and a dielectric constant less than 2.0. It acts as an effective weather seal, but is not insignificant when

considering RF transmission.

7.4 Design of Component Parts of Nosecone. For several reasons it was decided that the only feasible way to fabricate the nosecone was to make it in two halves. Although the radome only had to have a maximum angle of 160°, according to the requirements, the radome half of the nosecone had to be made larger than the back half in order to allow for tapering of the foam and fiberglass. Each of these tapers was two inches wide so that there is at least four inches all the way around the edge of the radome half of the nosecone (see Drawing 55131 D1056) which will not be well matched. As it was built the taper extends two inches on each side of the diametral plane. This means that the well matched portion of the radome, at the smaller end, subtends an angle of 164.5 degrees while at the larger end this angle is 170.5 degrees. This also means that the join line for the two halves is two inches on one side of the diametral plane. There is still another four inches of taper before the full thickness of fiberglass foam sandwich configuration starts again in the back half of the nosecone. Thus at any plane through the nosecone, perpendicular to the axis, the radome half had a 4 inch longer arc length than the back portion. Although there was no requirement that this back half be a radome, it was decided to construct the back half in the same manner as the radome was constructed, except that less care was taken in maintaining the accurate thickness of the foam. Also slightly

More resin was used to permit easier distribution of the resin into the cloth.

7.5 The Access Door. Largely to have the same coefficient of expansion as fiberglass, the access door was made out of a solid rolled sheet of stainless steel (Type 410) with an external covering of fiberglass. This fiberglass is primarily for esthetic reasons, to give the outside of the nosecone a uniform texture, but it also assists in our fabrication method for bonding the door in place. The door was screwed to a stainless steel frame (made of the same 14 guage stainless steel material) by means of 10-32 phillips head counter sunk screws on 2 inch centers. Riveted locking nut plates were attached to the back of the door frame. Holes in the door were precision match-drilled in order to provide integrity of structure. The door is appreciably heavier, per unit area (4 lbs/sq.ft.), than the rest of the nosecone, which typically has a weight of less than 1 lb./sq.ft. Because of the difficulty of making modifications to a sandwich type construction while still maintaining the general sandwich configuration, it was decided to make the rear side of the nosecone a solid laminate in the region where the access door was to be located. Unfortunately, two successive errors were made in the location of this door. Initially, the door was placed exactly opposite the center line of the radome and its location was then moved to an offset position. The door was completely fabricated and installed in the nosecone before it was realized that the offset had been made in the wrong direction. This error was due to a problem in visualizing the negative configuration of the nosecone when performing

the layout work in the mold. Although this error did cause a delay of a few days in delivery, it also offered the opportunity of examining the integrity of the sandwich structure. The structure was found to be very sound with excellent bond lines between the foam and the laminates.

7.6 Joining the Two Halves Together. Although each half of the nosecone was made as a foam fiberglass sandwich over most of its respective area, the join region was made of solid fiberglass. In some respects it would have been more desirable to keep the construction homogeneous throughout the nosecone (except in the access door region), but the problems associated with doing this did not justify that approach. In order to prevent high stress regions at the junction between the solid fiberglass and the sandwich regions, long tapers were used as has already been stated. There was two inches of foam taper (angle of 7 ^{o}) plus two inches of fiberglass skin taper (angle of 2.3") on each half, giving a total join width of 8 inches. It was felt that this wide join width was more than adequate to prevent any high or local stresses. The loads in the join material will be higher than the loads in the skins of the sandwich material, but since the thickness of fiberglass is appreciably higher in these regions, the net stress of the fiberglass material will be less. The total thickness of fiberglass in this region was at least .16 inches, or approximately half that of the total sandwich section and twice the total fiberglass thickness in these regions.

8. INTERFACE WITH THE NASA MOUNTING RING

It is obvious that an unmodified foam sandwich is not suitable for attachment to the aircraft, since the foam does not have adequate compressive strength. It was therefore necessary to fabricate this portion of the nosecone from a more solid material. The material used in this case was almost pure and solid fiberglass. Some small amount of filler material was added simply to obtian the correct dimension. While this material has somewhat lower strength than the fiberglass as far as tension is concerned, its compressive strength is quite comparable. A special tool had to be built to simulate the interface ring so that the inner surface of the nosecone could be molded to the correct shape to fit onto the process applied interface ring.

8.1 Design and Fabrication of Interface Simulation Tool.

It was decided to use a single triple purpose device for forming the inside interface surface of the nosecone, for providing for drilling the 40 interface bolt holes, and for closing off the nosecone in order to run the pressure tests to 11 psi. This device consisted of a fiberglass dome approximately 30 inches tall with a slightly flared skirt having an angle just over 8 degrees so that it fitted inside the nosecone without actually touching. The main structure was built from an existing mold which was approximately the right size. In order to get it up to the correct size, the skirt of the part was cut every few degrees and splayed out to a diameter approaching that of the NASA interface ring. (Drawing # 55131 D 1056). The slits were then patched

up with fiberglass and bearings were mounted at the top of the dome and also in the plywood disc placed in the bottom of the dome to spread the skirt out. These bearings were also obtained from a stock of precision tooling designed for our standard 3.250 inch "sweep shaft".

8.2 Generation of the Interface Surface. Using the existing HL precision tooling, the dome was arranged so that it could be rotated on the sweep shaft such that there was no more than two or three thousands of an inch possible freedom of motion for the dome except in the axial direction (where there would not normally be any movement due to the weight of the dome) and the freedom to rotate above the vertical axis. This configuration is shown in Fig.37. By rotating the dome about the precision 3.25 inch shaft and using our "sweep" techniques, a surface equivalent to the NASA interface ring was generated using a filled epoxy material which left a hard surface. The surface generated had the correct shape, but the diameter was .040 inches larger than the NASA interface ring for reasons which will be explained later. This mold surface could now be released and used to mold the inside surface of the nosecone.

8.3 Molding of Interface on Nosecone. The interface region of the nosecone was prepared by grinding away all superfluous fiberglass material which built up during the initial fabrication of the nosecone. This consisted of lumps of resin and excess fiberglass coating where there was overlapping in the joining of the two halves, etc.

The problem here is to obtain a finished part which has a finished surface on both the outside and inside surfaces. In this case the inside molded surface is more important since it has to interface with the aircraft (ring). This region only extends in about 1.5 inches and the rest of the inside of the nosecone will end up with a fiberglass textured surface of undefined surface finish.

After placing the nosecone thus prepared onto the endcap mold to ensure that there was no interference, an epoxy filled material was spread onto the interface region and the whole nosecone put back on the endcap mold in order to mold the interface surface. This mold material is an epoxy mixture which has a strength womewhat less than fiberglass and is therefore not entirely desirable as the actual interface material, especially since it would be in compression at the bolt holes when the nosecone was pressurized. Consequently, when this mold material had cured and the nosecone was removed from its mold, additional mold material was added together with three layers of fiberglass tape (.030 inches thick) and the whole nosecone replaced on the mold. The diameter will now obviously be smaller than the mold by .06 inches, so that the nosecone will not fit all the way. Since the mold was made with a .04 inch larger diameter (as already stated) than the NASA made interface ring, the nosecone will end up with a diameter of about .02 inches smaller - depending on the temperature. Since the

slope of the interface surface is 1 in 7 (each side), the nosecone will slide onto the interface surface to within .07 inches of the stop. If it is forced on so as to stretch the fiberglass and compress the aluminum interface ring slightly, a gap of approximately .05 inches will result between the radial surface of the interface ring and the end of the nosecone, which is the amount requested by NASA personnel at a meeting at JSC, Houston, on 17 August 77.

9. AERONAUTICAL ANALYSIS

The complete analysis appears as Appendix "A" to this report. Documents which were supplied by NASA relating to the flight profile were used to determine the ultimate loading. These were used in conjunction with MIL-S-5705 (USAF) as called out in the NASA documents. This data offered sufficient basis upon which to establish a set of loading conditions for design of a nosecone suitable and safe for the intended use. Using these conditions and the theoretical methods described briefly below, aerodynamic pressures, loadings, shear and bending moments were tabulated. The schedule of pressurization was used as the design conditions for the analysis of forces and pressures from design conditions for the analysis of forces and pressures from that source. Inertial loads, shears and moments were formulated as a separate set of requirements.

Examination of flight conditions would indicate that the nosecone will not encounter temperatures in excess of those on the ground on a hot day and that analysis of thermal loading in flight is unnecessary, except for consideration of the thermal

gradients present when flying at 60,000 feet (up to 130-150°F).

Structural pressures and loads were divided into categories. They consist of those generated by the following:

a) The nosecone's shape

b) Its inclination to the airstream

c) Pressurization

d) Inertial forces.

The velocities and pressures about the basic shape were determined with respect to free stream conditions using potential flow theory. By means of distributed sources and sinks a body of revolution very closely approximating the shape of the nosecome was created and the potential flow about it calculated. This part of the loads analysis can be completed rapidly when the maximum free-stream dynamic pressure for the aircraft is known.

The pressures, forces and moments arising from airstream inclination were calculated for an arbitrary angle of attack using an adaptation of the theory of the Reference.

This data was then used to perform a mechanical analysis.

10. MECHANICAL ANALYSIS

Data obtained from the aeronautical analysis and the RF design of the radome were analyzed to ensure that all stresses and loading were acceptable. The analysis is included as Appendix B.

In summary, the stresses in the fiberglass and foam are all well within the allowable stresses to handle the anticipated loads.

The analysis was done originally for the access door approximately in the middle of the nosecone, but the stresses are so low that moving the door to a location nearer the aircraft does not materially effect the results of the analysis.

10.1 Low Temperature Tests. Structural failure tests were performed on a number of samples of sandwich with exactly the same configuration as was used in the nosecone, except that the samples were flat. Tests were performed at room temperature and in contact with dry ice which sublimes at -79°C (-110°F). These tests were primarily to check the resistance to shear of the foam. It was found that the failure strength at the low temperature, which is assumed to be -80 to -100°F just inside the sandwich, was consistently 50% of that at room temperature. However, both values were well above the loads to be encountered in operation.

11. ANCILLARY FABRICATION EQUIPMENT

Two pieces of special fabrication equipment were needed to machine the foam core material. This was made in gores each equal to 1/16 of the complete nosecone area. Thus each piece was 8.5' long and 9.5" at its widest point. The outside edges of the foam core of each half had to be tapered down to nothing over a 2 inch distance.

11.1 The Thickness Planer. A piece of Hacking Lab's equipment was modified to allow the gores of foam, which had previously been cut to a thickness of approximately .31", to be uniformly

and accurately machined down to a thickness of .250" ± .005. The best pieces were chosen for the radome and those with some irregularities were used for the back portion of the nosecone where exact thickness was not so important. The plane used rotating rollers fitted with appropriately fine sandpaper and motor driven.

11.2 The Edge Taper Cutter. This was a much smaller device operating on the same principle, but with only one small roller-sander. It could taper the foam down to a feather edge.

12. POST CURE

In order to ensure maximum strength and stability to the nosecone it was "post cured" for several hours at a temperature of at least 160°F. A temporary insulated oven was built to accomodate the complete nosecone (after all epoxy work was finished). A circulating fan and thermostatic control was included. Due to the vessel type configuration of the unit which tended to prevent the free flow of air, the temperature inside the nosecone was no doubt appreciably higher than the control temperature at the bottom of the oven, but this assured that every part of the nosecone was soaked at a temperature of at least 160°F.

13. ADDED EQUIPMENT

Two items of GFE were mounted in the finished nosecone. These were a glide slope antenna (GSA) and a total air temperature sensor (TATS).

13.1 The GSA

This unit had a metal base 4.5 X 2 inches with 6 countersunk mounting holes and a type N(F) connector. A fiberglass

bracket was designed and fabricated and was later bonded to and integrated with the nosecone so that the GSA would be near the top in the forward end and sloping down at an angle of approximately 30 degrees. After curing, the GSA was mounted in place. No tests were performed on this unit except for physical inspection and a hand applied load to ensure that there was no grossly poor bond.

13.2 The TATS

This unit was mounted approximately half way along the nosecone in the middle of the join between the radome and back section. An aluminum disc was mounted inside the nosecone to help distribute the local loads which could be high if the TATS were inadvertently banged. Placing it in this location ensured that no cutting or drilling into the relatively delicate foam sandwich matrerial was necessary.

The TATS supplied for mounting was used as a mold to form a loading eposy mounting surface. There is, therefore, an extremely good fit between this particular TATS and the hole in the nosecone.

14. RF TESTS

The purpose of these tests is to measure the transmission loss through the radome as a function of position on the radome, angle of incidence and polarization.

14.1 Test Fixture. A test fixture was built for measuring the transmission through the radome before the radome was bonded to the back half of the nosecone. The test fixture is shown in Fig. 7 from which it can be seen that the radome

axis is vertical. The transmitting generator, which was set at a fixed frequency of 9.6 GHz, was rigidly attached to the transmitting horn through a precision attenuator which was used for calibration of the chart recorder pen. The transmitting generator acted as a counterweight to the receiving horn and its support structure. This horn maintained a constant relationship with the transmitting horn, and the whole unit could be adapted to different elevation angles apart from the horizontal orientation shown in Fig. 7. These angles of 6^{o} represent the limits of excursion of the side looking radar with respect to the nosecone. Since the nosecone has a conical angle of 8^{o} (to the axis of rotation) it can be seen that the transmitted energy never has a direct path to the receiving horn which is perpendicular to the radome. For all the tests the angle of incidents was either 2^{o}, 8^{o}, or 14^{o}. The whole RF measuring structure could be moved up and down in increments of 4 inches and could also be moved sideways by up to 7" from the diametral plane. Polarization could also be rotated.

It should be noted that since the radius is the RF structure pivot center to the radome is approximately 49", a 6^{o} tilt represents a vertical rise of approximately 5.1" which is not very different from the vertical separation between the various measurement heights. Thus approximately the same region of the radome is illuminated as the RF structure is moved up one increment and tilted down by one increment.

14.2 Test Results. Because of the large area of the radome and different angles of incidence, polarization angle and offset from the diametral plane, a large amount of data was gathered. Most of it is included in this report, but it by no means is a complete map of the whole radome area and certainly does not cover all combinations and permutations of the variables.

Some of the data is repeated, either intentionally or accidentally, but where this occurs it is useful in providing a measure of the repeatability of the data.

Each figure generally contains data for angles of incidence of 2^{o} (labeled $+6^{o}$), $8^{o}(0^{o})$ and 14^{o} (-6^{o}) and it can be seen that in general the "worst" data occurs at 2^{o}, and would probably be even worse at normal incidence 0^{o}. This is to be expected because in that case energy would be reflected right back causing the most severe standing waves and, therefore, disturbances to the measured data.

In each case, at least two records are superimposed. The test fixture was displaced by a quarter wavelength (.30") between each such pair. The appropriate "correct" curve for each set of data should be construed as the average of the two. It whould be noted that the actual curves obtained are a function of the exact distance of the test fixture antennas from the radome. Because two curves track each other well, does not necessarily mean that if the test fixture had been displaced 1/8 wavelength that the two curves would not be

separated appreciably, and vice versa. The mean curve should however be the same in both cases.

Each record is labelled with four pieces of information listed below

a) The height of the pivot point above the base, in inches.

b) The angle of the waveguide to the horizontal.

c) The polarization, either parallel ($\parallel$) or perpendicular ($\perp$) to the nosecone axis.

d) The amount that the horns are off-set, above or below the diametral plane (assuming the axis is horizontal).

14.3 Calibration of Data. In each case the attenuation as measured with a precision waveguide attenuator was adjusted to a value of .2dB/inch with the zero level being set for direct transmission with no radome in place. In all cases the left hand region of the record corresponds to the upper portion of the radome, and the scale is 22.5°/inch.

14.4 Restriction of Travel. Since the radome half subtended an average angle of about 190°, and the size of the precision attenuator created a dead angle of about 17°, the maximum angle through which the radome could be rotated was

$$(360^\circ - 190^\circ) - 17^\circ = 153^\circ$$

This angle was even less when the antennas were offset from the diametral plane and in addition part of the scan angle is taken up with scanning through the tapered edge of the radome. This effect is quite dramatic on the recorded data.

14.5 Transmission Data. The strip chart recordings of the transmitted signal are shown in Figs. 8 thru 36.

14.6 Specific Points of Interest. Due to the size of the radome it is not possible to get glass fabric big enough to make it all in one piece so each of the 4 layers of each skin had to be made in 2 pieces. The cloth width was 38" and a 2" wide overlap joint was used for each piece such that no joints overlapped, but they were contiguous. Thus, the maximum number of layers was five (on each laminate). The joint region therefore extended from approximately 30 to 38" from the open end of the nosecone. In addition, the method of distributing the resin by hand tended to leave an accumulation at the edges. Consequently in this region the laminates are not only at least 25% thicker, but contain variable amounts of excess resin. As a consequence, it is to be expected that the transmission data obtained from this region will be somewhat different from that obtained over most of the radome. As a consequence, a relatively large amount of data was obtained relating to this region which includes 29", $+6^{o}$ and 41", -6^{o}, although the effects at this latter combination are less noticable due to the high incidence angle and therefore, reduced energy reflected back into the antennas.

Another region which is of particular interest is where a narrow patch of glass fabric, one ply thick, and about 2-3 inches wide, giving a total of 5 plies for the outer skin, had to be applied during fabrication. It has a very dramatic

effect which is obvious in Figs. 33 and 36, about 2" from the left of the records for 61", +6° and 65", 0°.

It is especially apparent on the recorded data because the patch is so narrow and therefore has a focusing effect, not only producing an apparent increase in attenuation, but also an apparently lower attenuation than anywhere else on the respective record. This apparent effect is almost certainly not real, but the ripples produced by this one extra ply of fiberglass do give perspective to the other ripples occurring on the records.

Creases on the inside fiberglass skin could also be identified with ripples in the data. Care was taken not to remove these creases to improve appearance, since this could compromise the strength of the nosecone.

14.7 Effect of Moving Test Fixture by Quarter-Wavelength. In Fig 20 for 33",0°, the effect of moving the RF measuring structure a quarter-wavelength to obtain an average transmission characteristic is dramatically demonstrated. In this record, the structure was set in a third position which was a half wavelength from the first, resulting in an almost identical record (except for some slight anglular displacement due to experimental error).

The fact that the quarterwavelength spaced curves cross over (as they do in several other records) is probably indicative of the fact that although the radome was set up to rotate about its own axis, it was not rigid enough, without the

rest of the nosecone, to maintain a circular shape. This results in the distance between horns and radome changing as a function of rotation. This change need only be a total of .3" to give the effect shown in Fig. 20 33", 0^{o}.

14.8 Summary of Data. In general the apparent transmission loss varies between .1 and .3dB although it does appear to go to nearly .5dB in some of the regions discussed above.

In the offset cases the attenuation appears to be over 1dB in some cases in the tapered region at the edge of the radome. This measurement has little meaning, but what is significant on most of these offset records is that beyond the tapered region there is nothing between the two antennas and the attenuation can be seen to be 0dB, within the stability of the measuring equipment, approximately .02dB.

15. PRESSURE TEST

As is shown in the aeronautical analysis, the nosecone should be designed to handle an ultimate pressure of 11 psi. A test was performed to show that the finished nosecone (unpainted) could survive, such a pressure without damage.

15.1 Test Configuration. Fig. 37 shows the test set-up. The pressure guage was previously calibrated against a water manometer with a 24 ft. head and found to be accurate to within 2%.

Since the test personnel were located some distance from the unit under test for safety reasons, a separate air line was run from the vessel with only the pressure guage attached to

it. This insured that the measured pressure in the vessel was not a function of the leak rate.

The nosecone was bolted to the interface tool (end cap) with standard aircraft-type .250 nuts and bolts which fitted tightly in the 40 holes. A silicone sealer was used to seal the interface.

The TATS was fitted to the nosecone for this test.

15.2 Test Results. The pressure was increased gradually and held at 6-7 psi for about 15 mins. Some leaks in the end closing had to be repaired. The pressure was then slowly taken up to 11 psi. It was not held for more than two minutes before there was a failure of the end cap which produced a leak too large to maintain the air pressure. The test was declared satisfactory.

Examination of the nosecone after the test showed no apparent change or damage. Since the nosecone had not been painted, any fracture of the fiberglass or separation from the foam would show up as a lighter coler since the fiberglass laminates are relatively transparent, except where air spaces occur, such as at fractures.

16. FINISHING

Since it had been agreed that NASA would paint the nosecone, it was merely wiped with a thin layer of epoxy resin to fill any small voids and sanded smooth, preparatory to packing and shipping.

17. CONCLUSIONS AND SUMMARY

The nosecone was successfully designed, fabricated and tested, mechanically, to its ultimate design loading requirement in accordance with certain USAF specifications. It was also tested for RF transmission at the operating frequency of its intended side looking radar (9.6 GHz) and found to have less than .5dB attenuation (generally considerably less) for a wide variety of angles of incidence, polarization, offsets and positions in the radome. There were no apparent weak points.

The weight, at approximately 100 lbs., was very low for such a large structure.

Cross Sectional View

Name.

Reflection Characteristic

Voltage —— , Power - - - -

a)

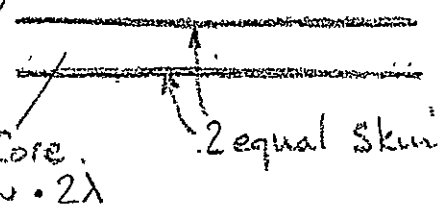

Core ~ .2λ

2 equal Skins

Quarter Wave "A" Sandwich

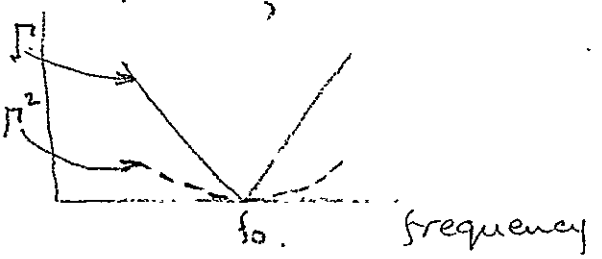

b)

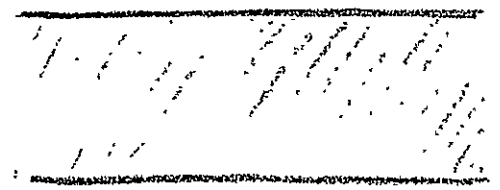

Core ~ .7λ. 2 equal Skins

3/4 Wave "A" Sandwich

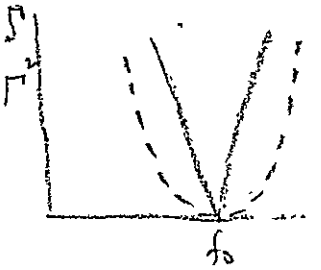

c).

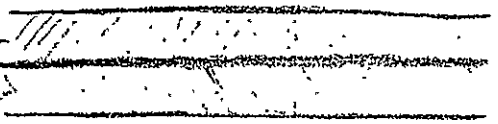

Cores. ~.2λ each

Inner & outer skins equal

Center skin ~ 1.8 times as thick

3 Skin quarter Wave Sandwich ("C" Sandwich)

d)

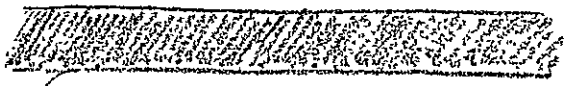

Single Layer Solid Fiberglass ~ .25λ. (for ε = 4 ε₀).

Half Wave Single Layer.

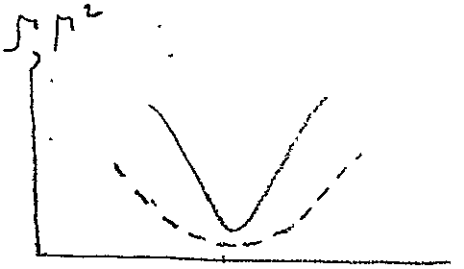

ORIGINAL PAGE IS
OF POOR QUALITY

Fig 1. Some Matched Radome Configurations

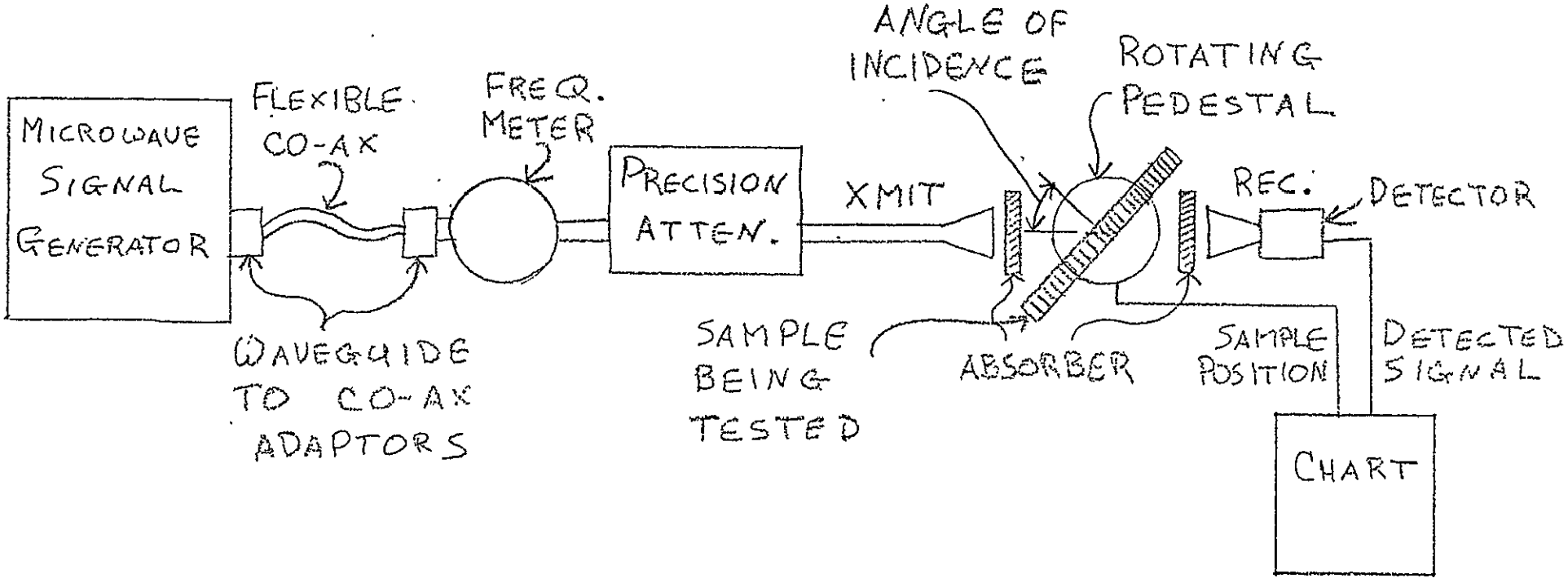

Fig 2 Set up for testing Flat Samples.

ORIGINAL PAGE IS
OF POOR QUALITY

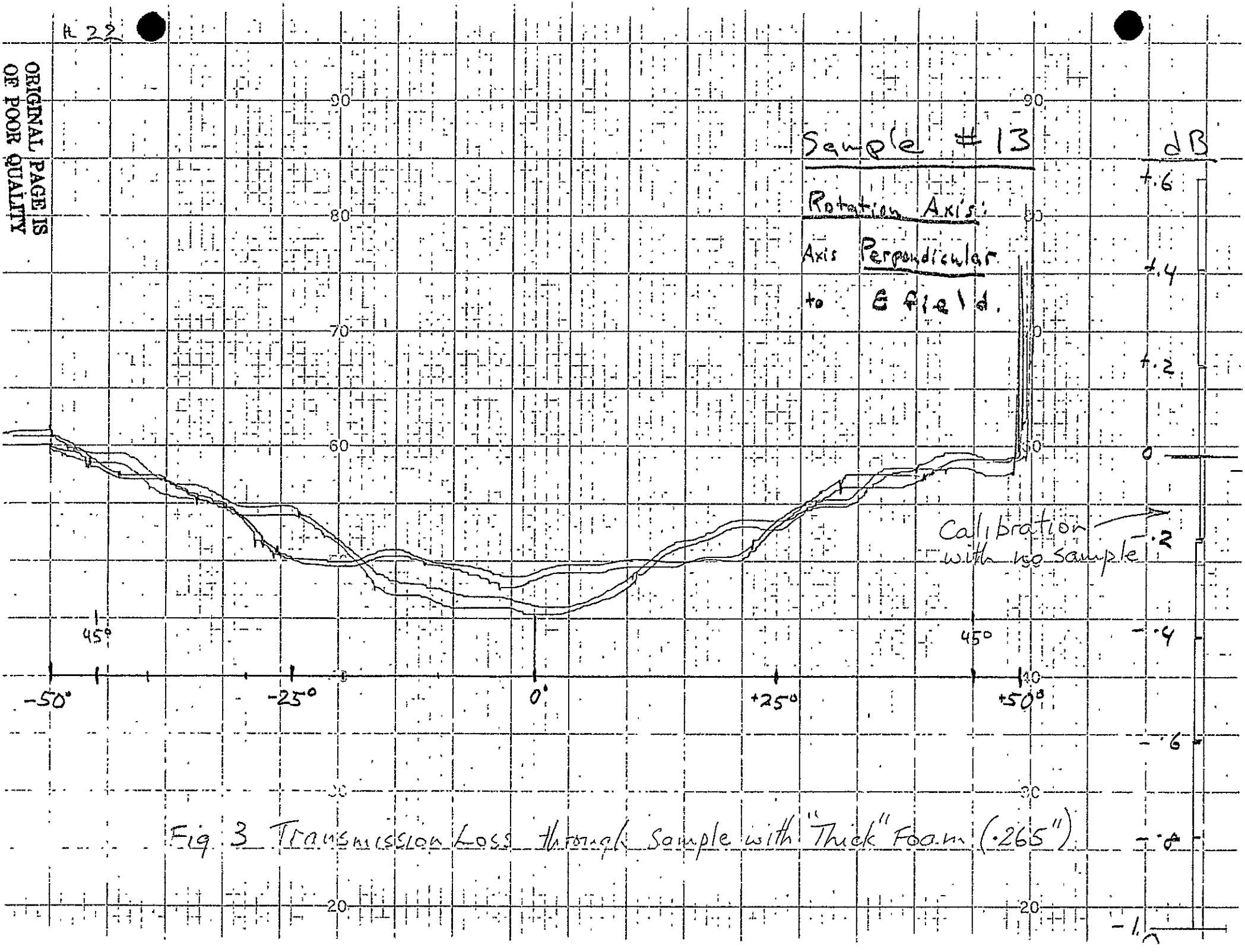

Fig. 3 Transmission Loss through Sample with "Thick" Foam (.265")

H:22

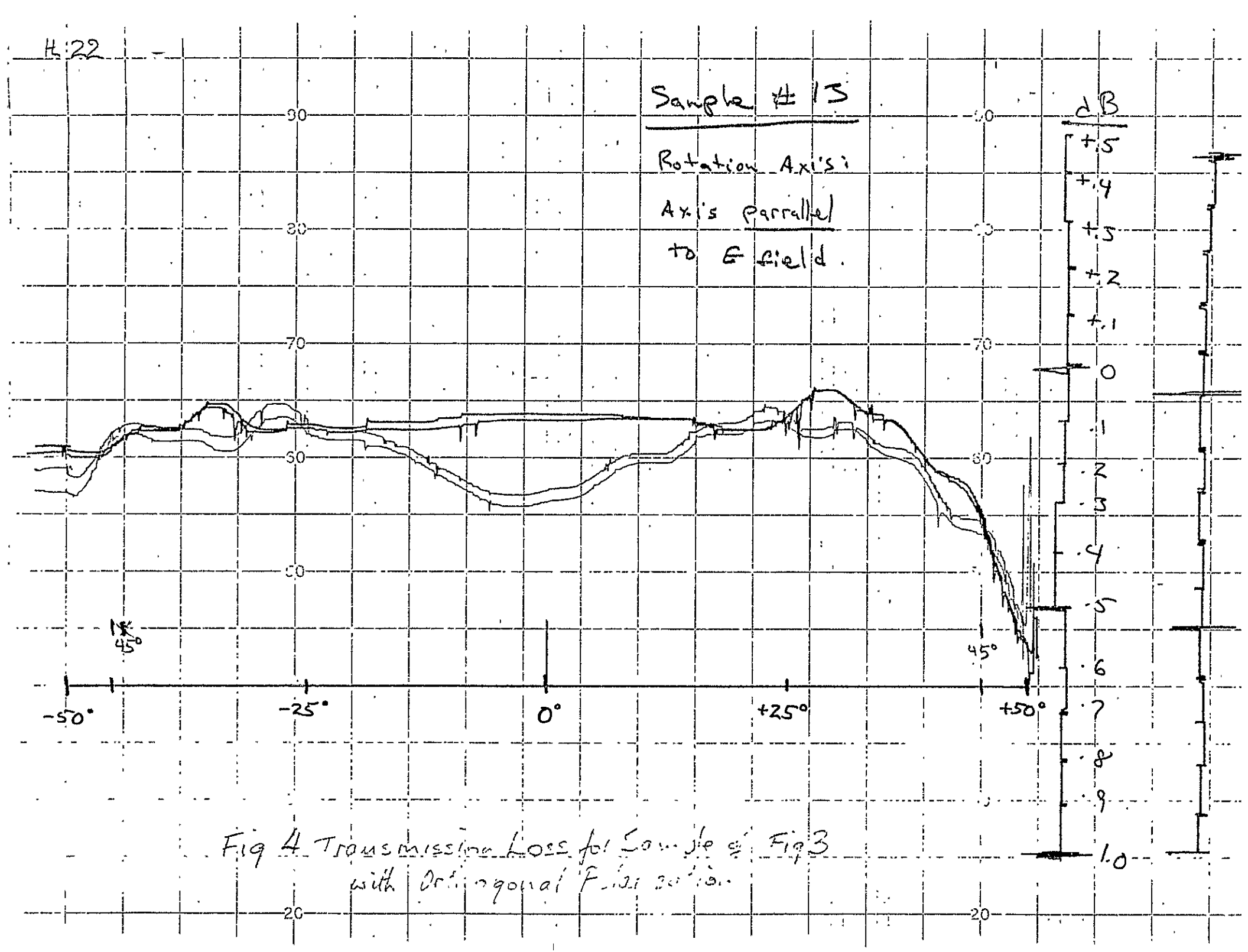

Fig 4 Transmission Loss for Sample of Fig 3 with Orthogonal Polarization.

ORIGINAL PAGE IS
OF POOR QUALITY

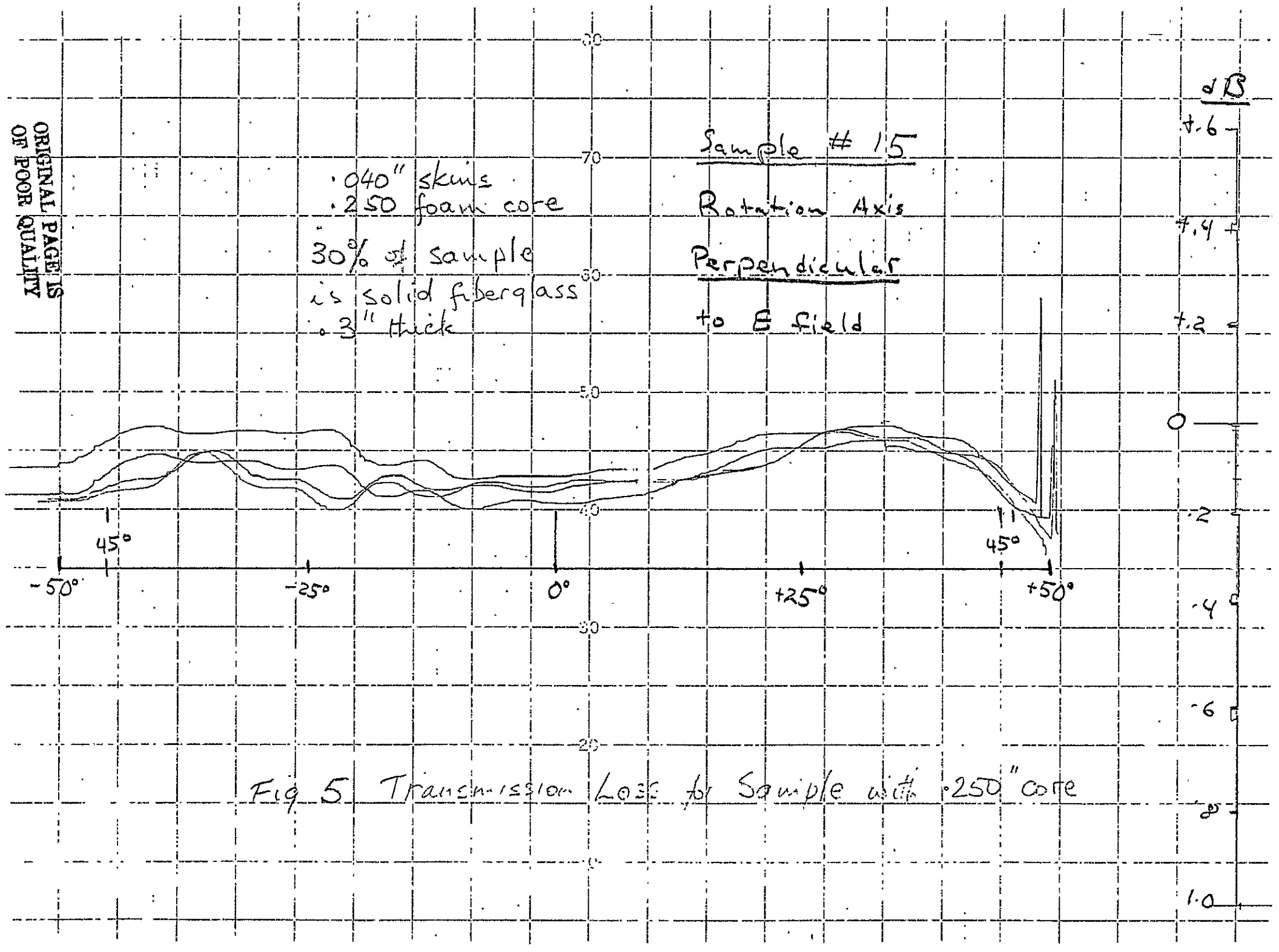

Fig 5 Transmission Loss for Sample with .250" core

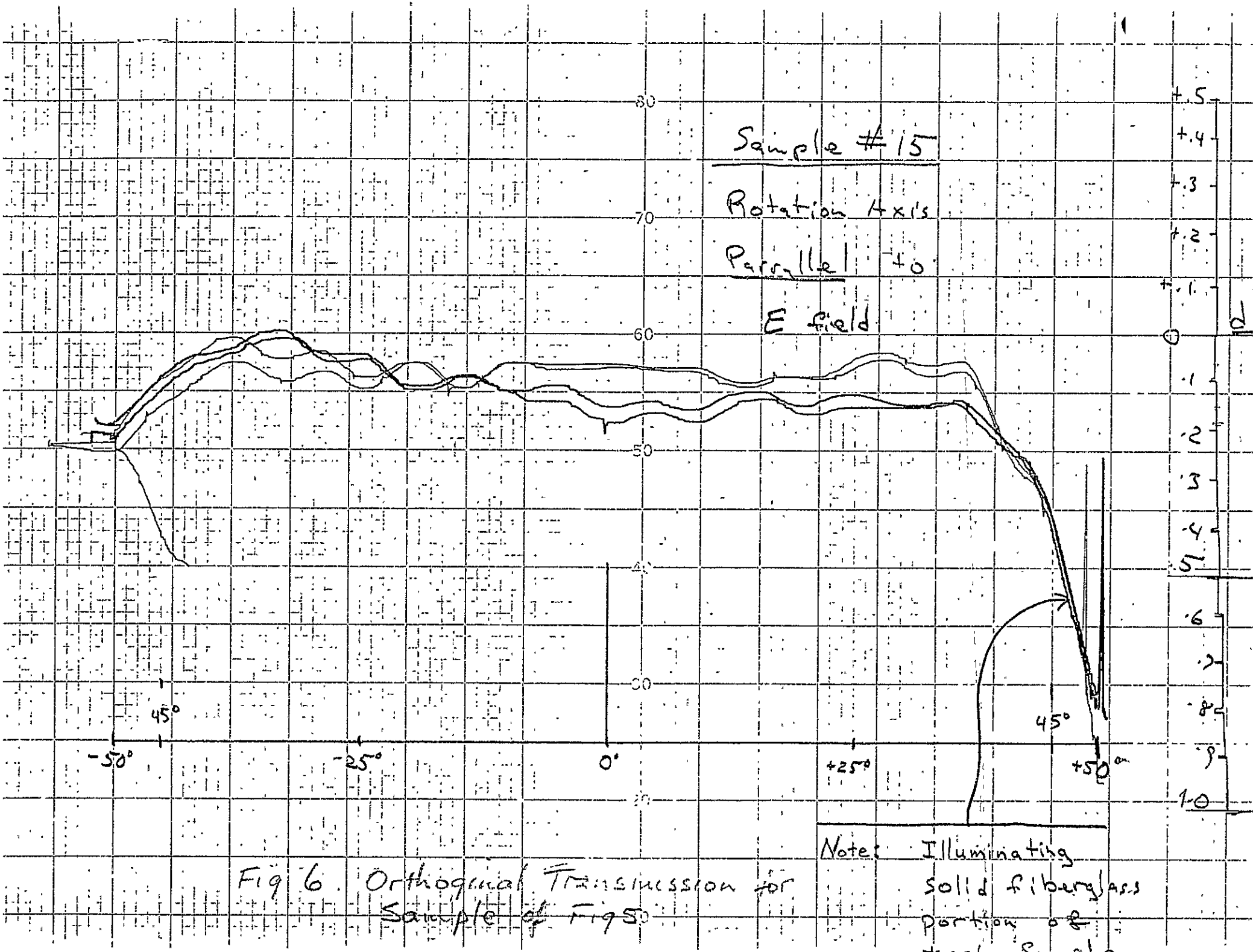

Fig 6. Orthogonal Transmission for Sample of Fig 5

ORIGINAL PAGE IS
OF POOR QUALITY

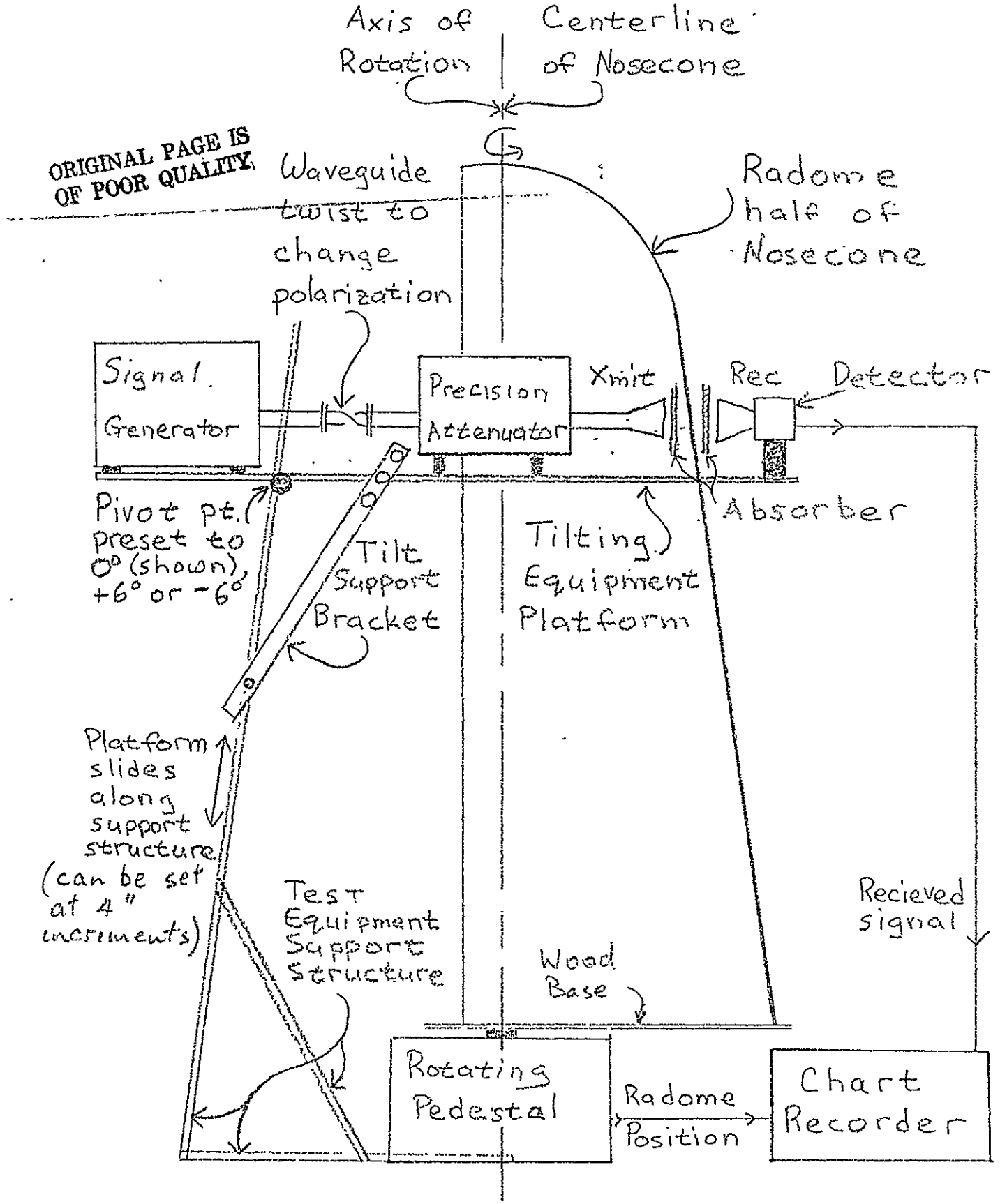

Fig. 7 Test Fixture for Measuring Radome Transmission

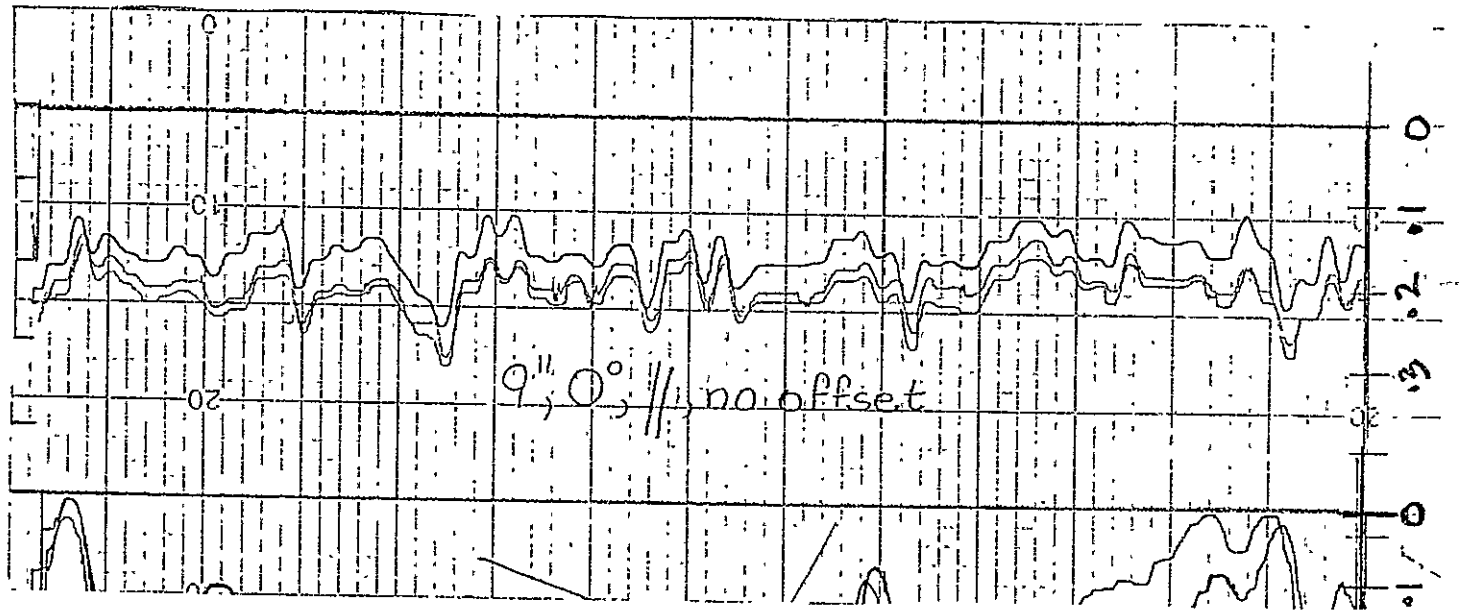

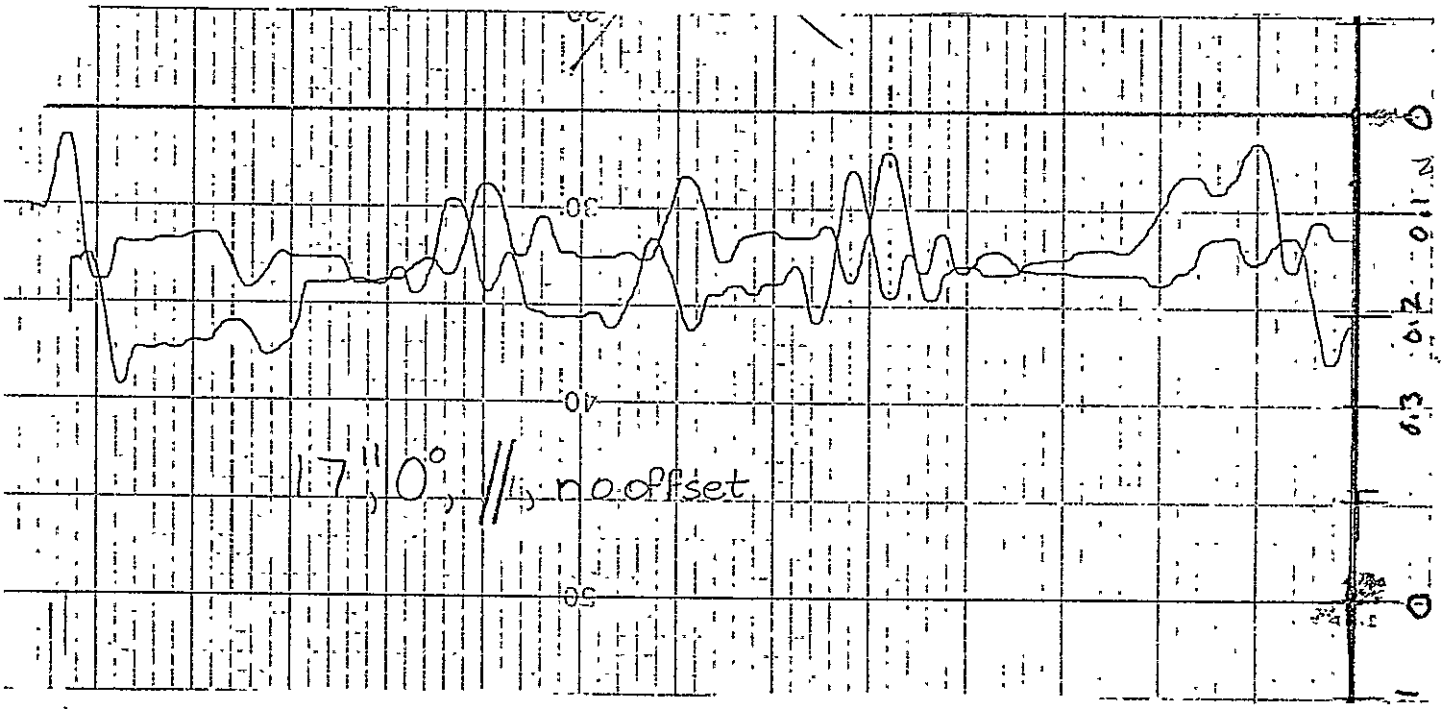

Fig 8

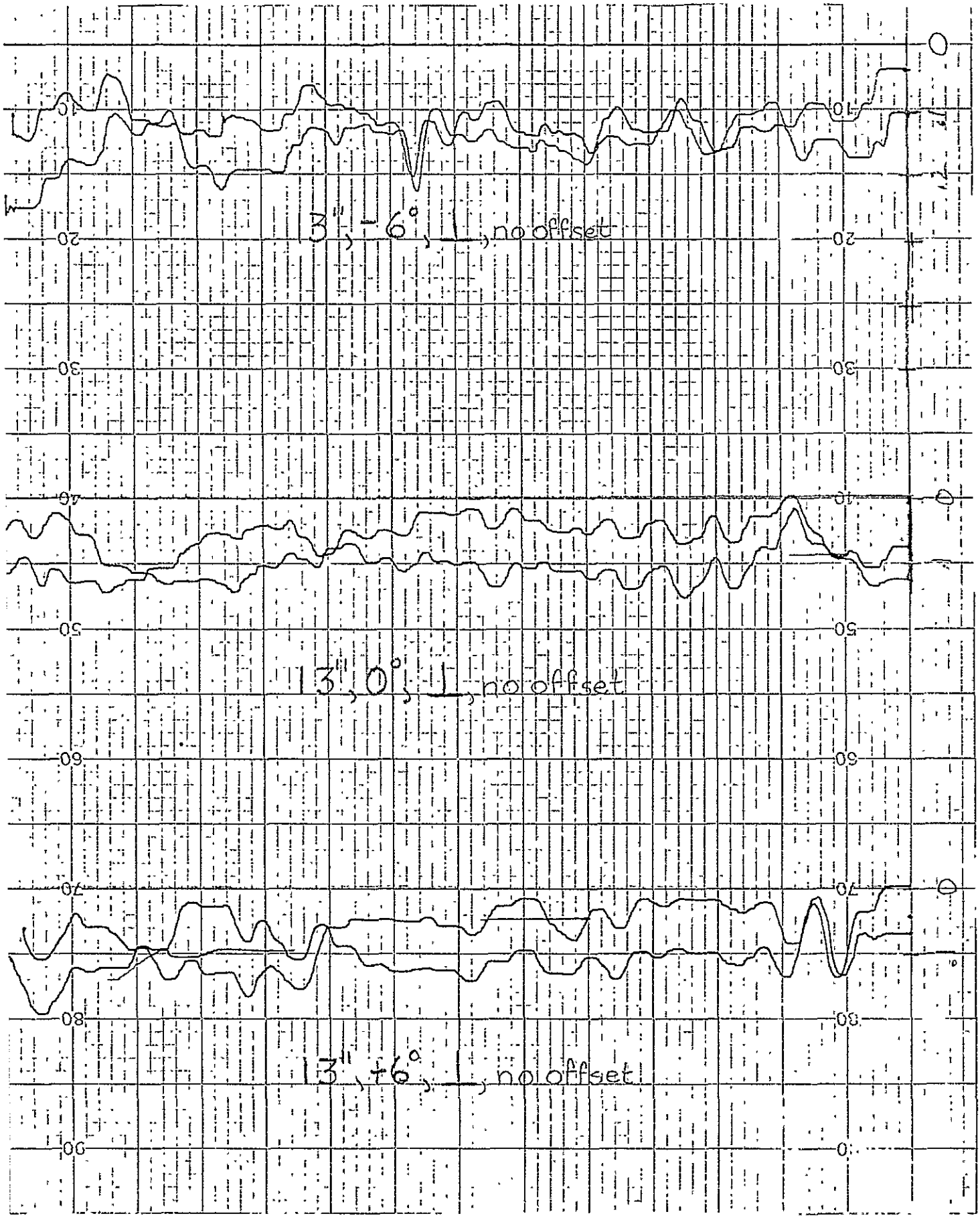

Fig 9

ORIGINAL PAGE IS
OF POOR QUALITY

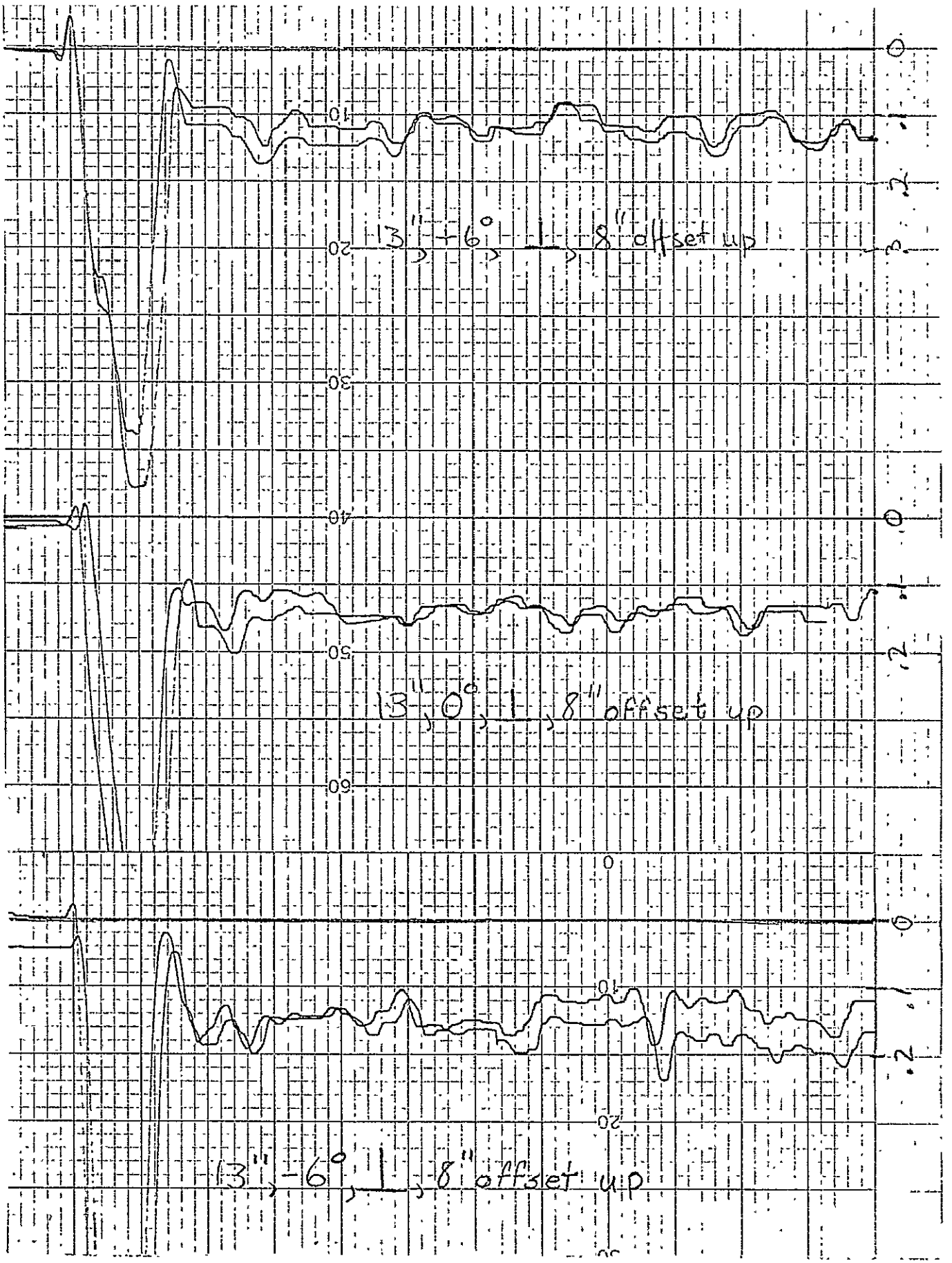

Fig 10

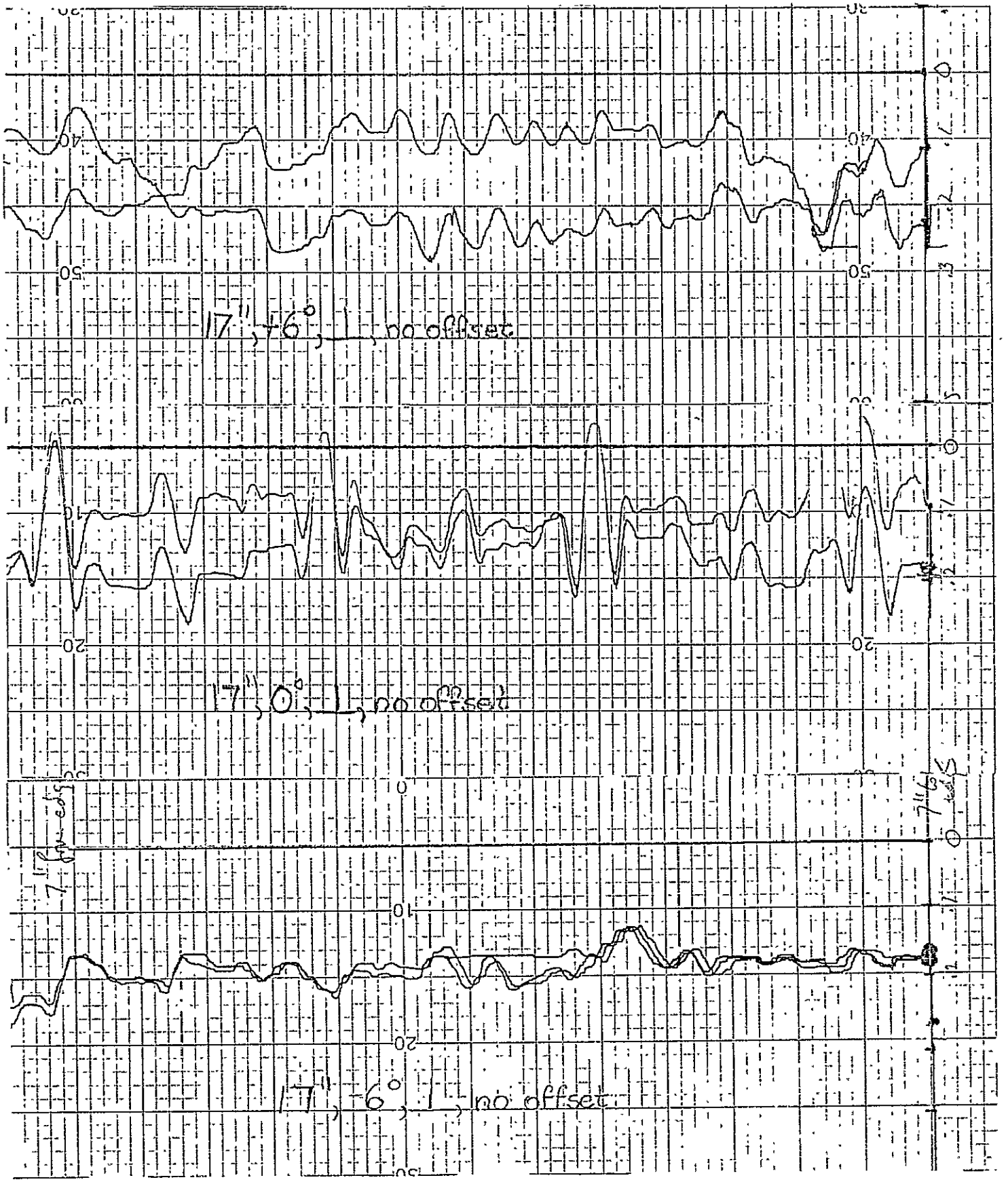

Fig 11

ORIGINAL PAGE IS
OF POOR QUALITY

Fig 12

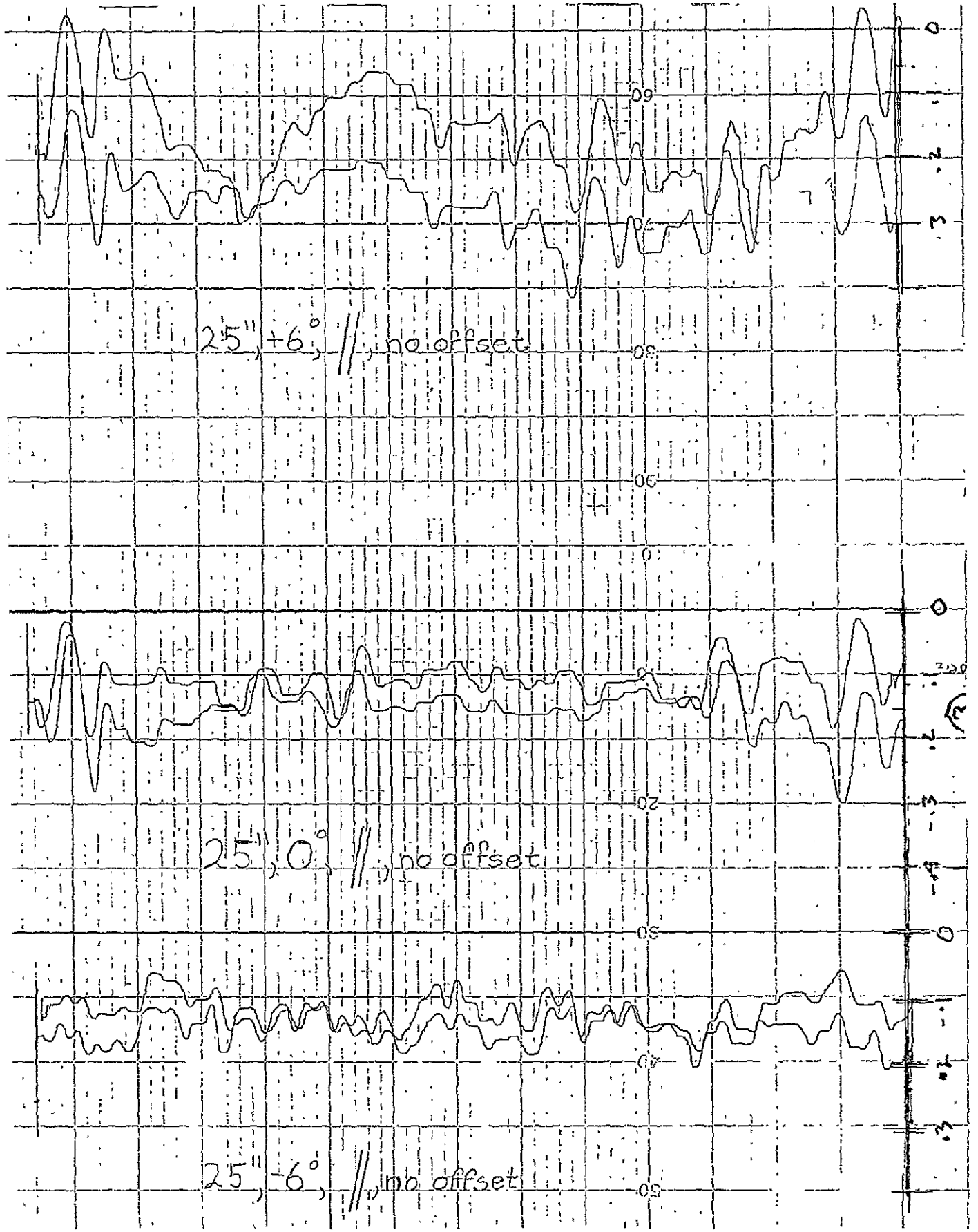

Fig 13

ORIGINAL PAGE IS
OF POOR QUALITY

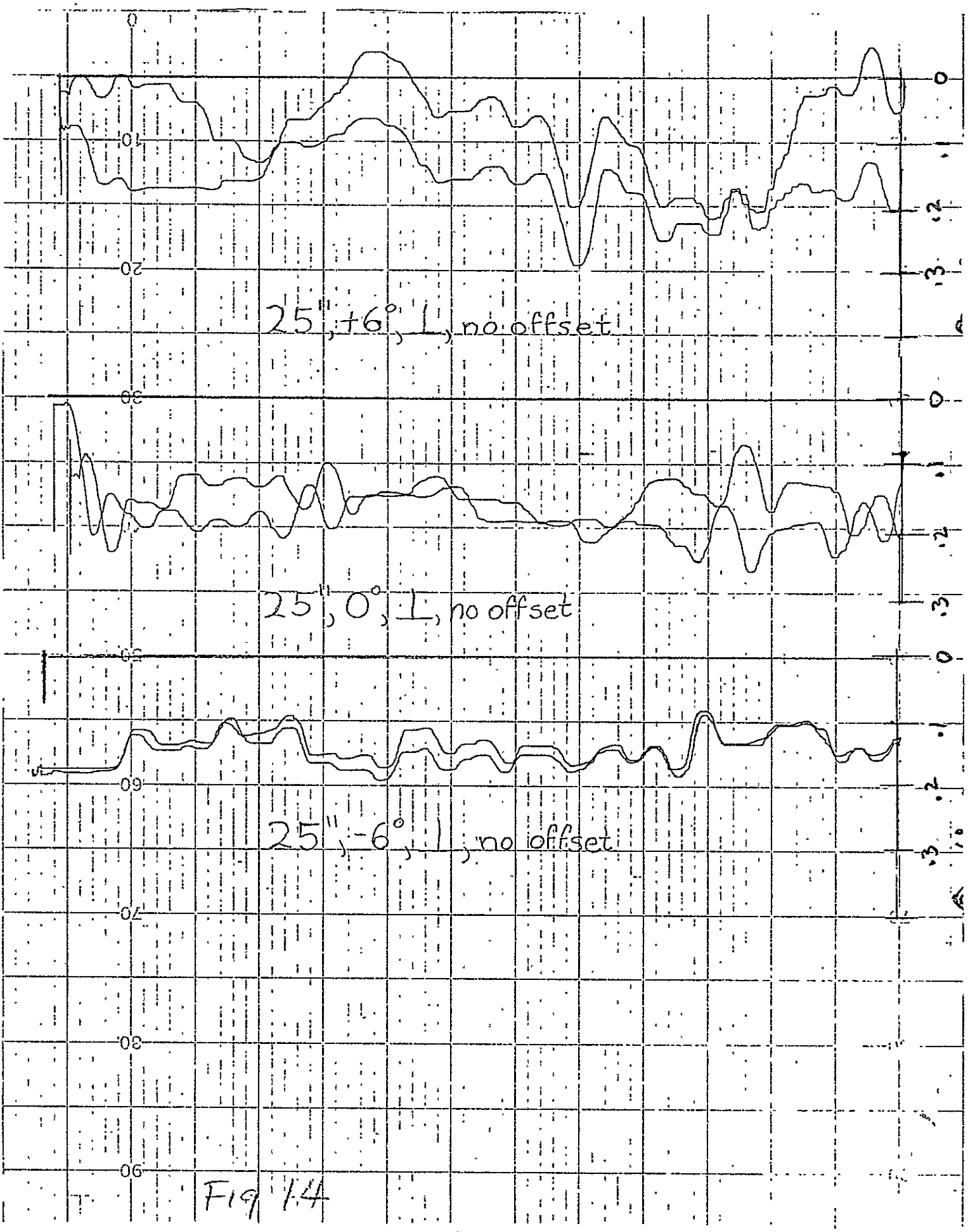

Fig 14

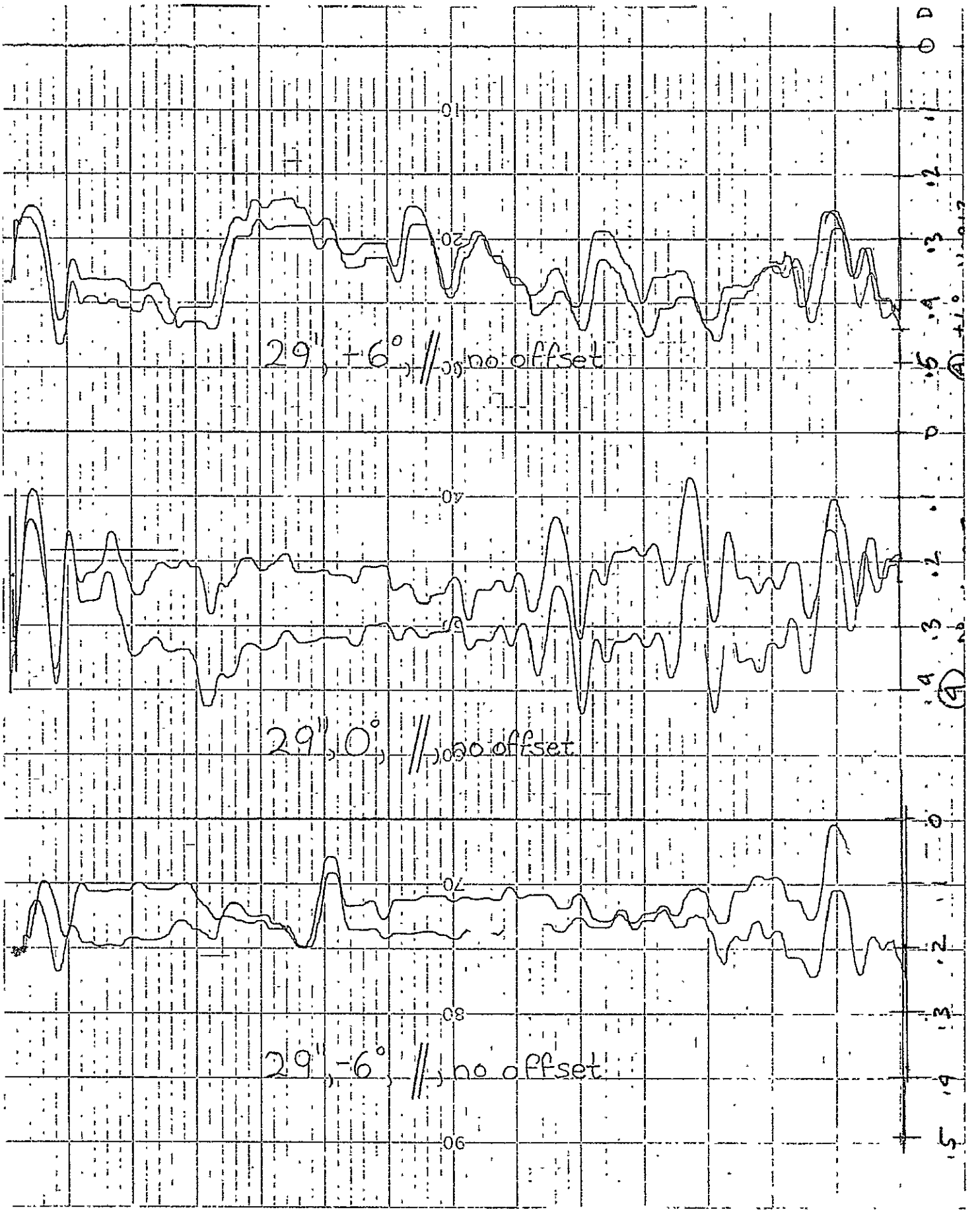

Fig 15

ORIGINAL PAGE IS
OF POOR QUALITY

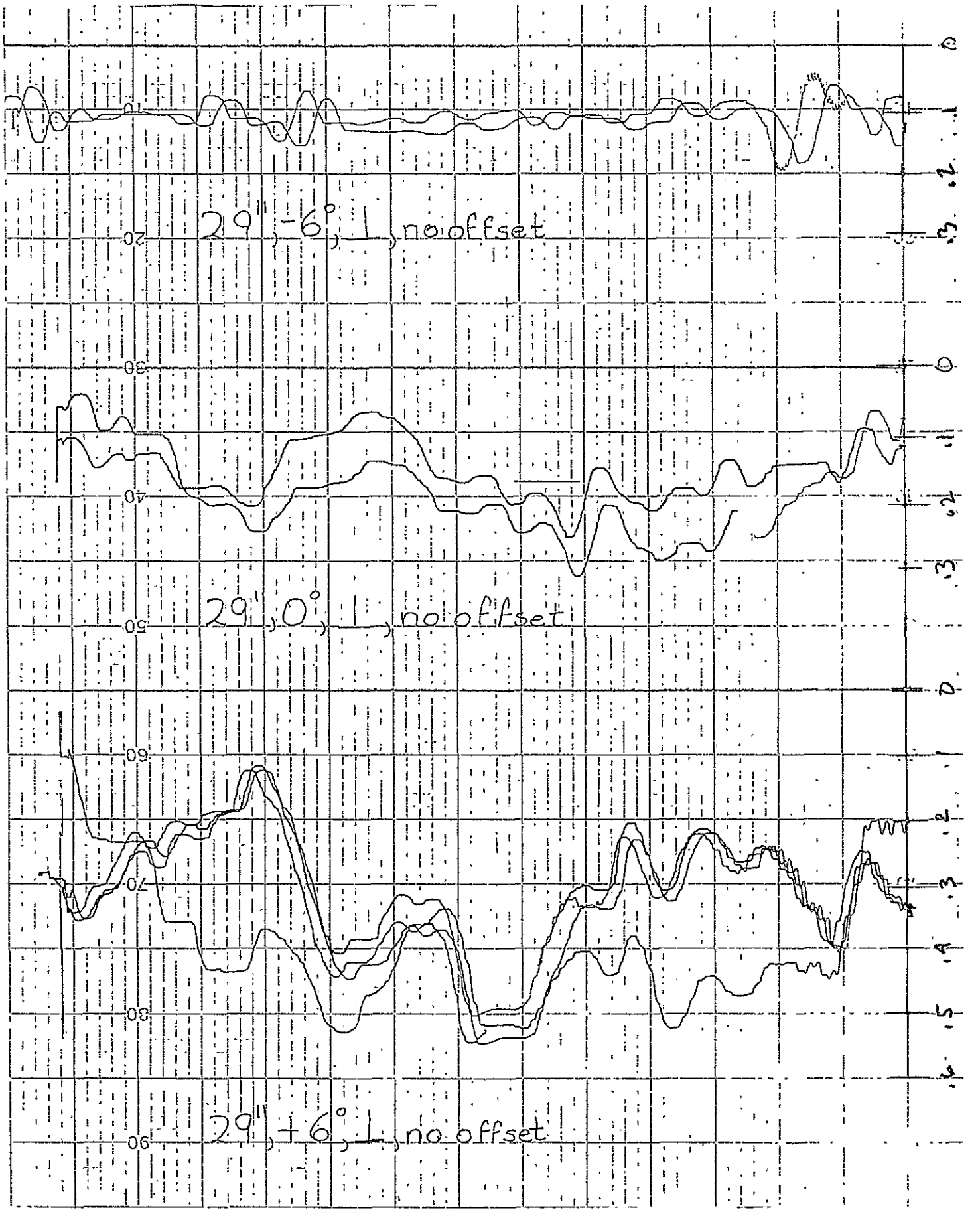

Fig 16

Fig. 17

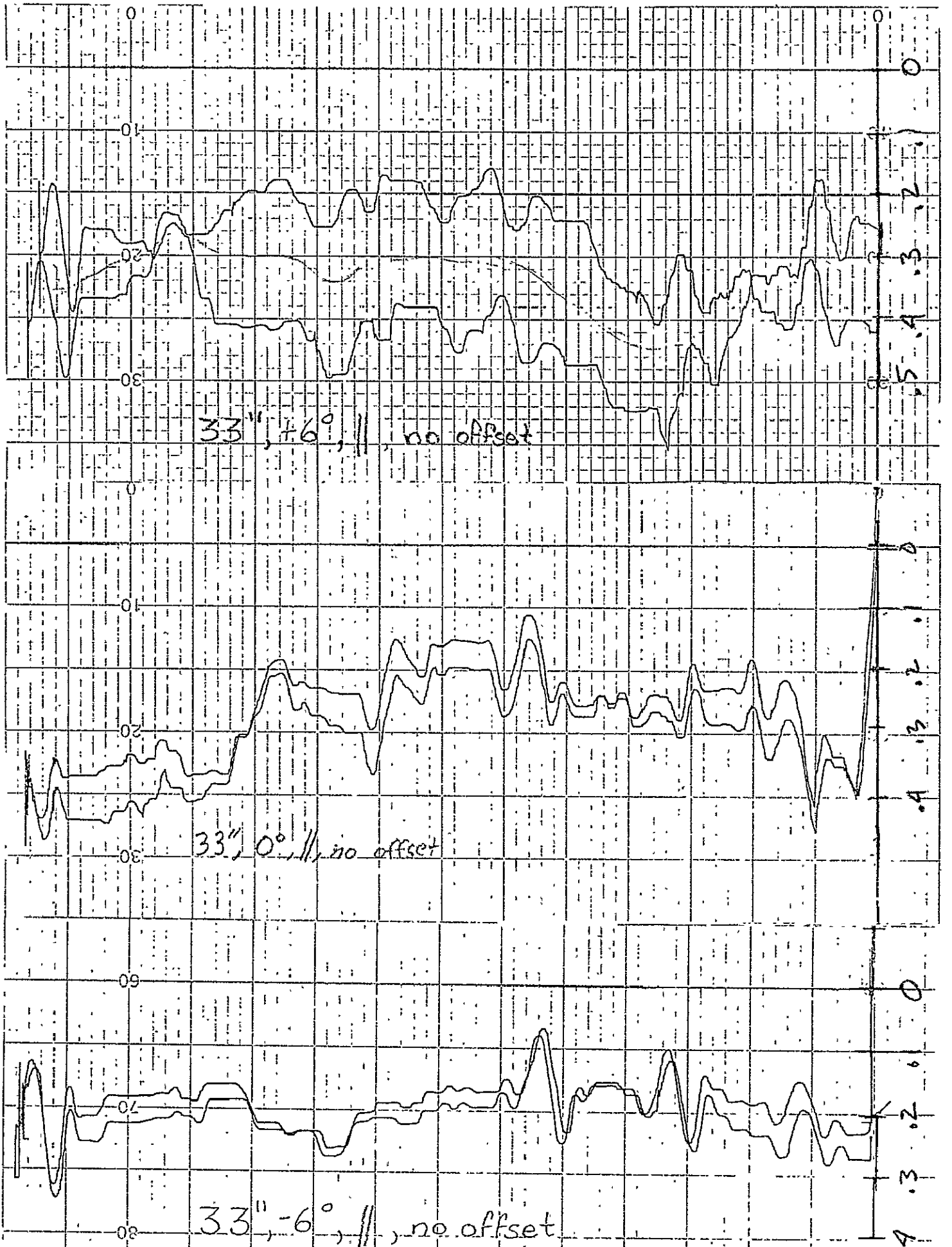

Fig 18

ORIGINAL PAGE IS
OF POOR QUALITY

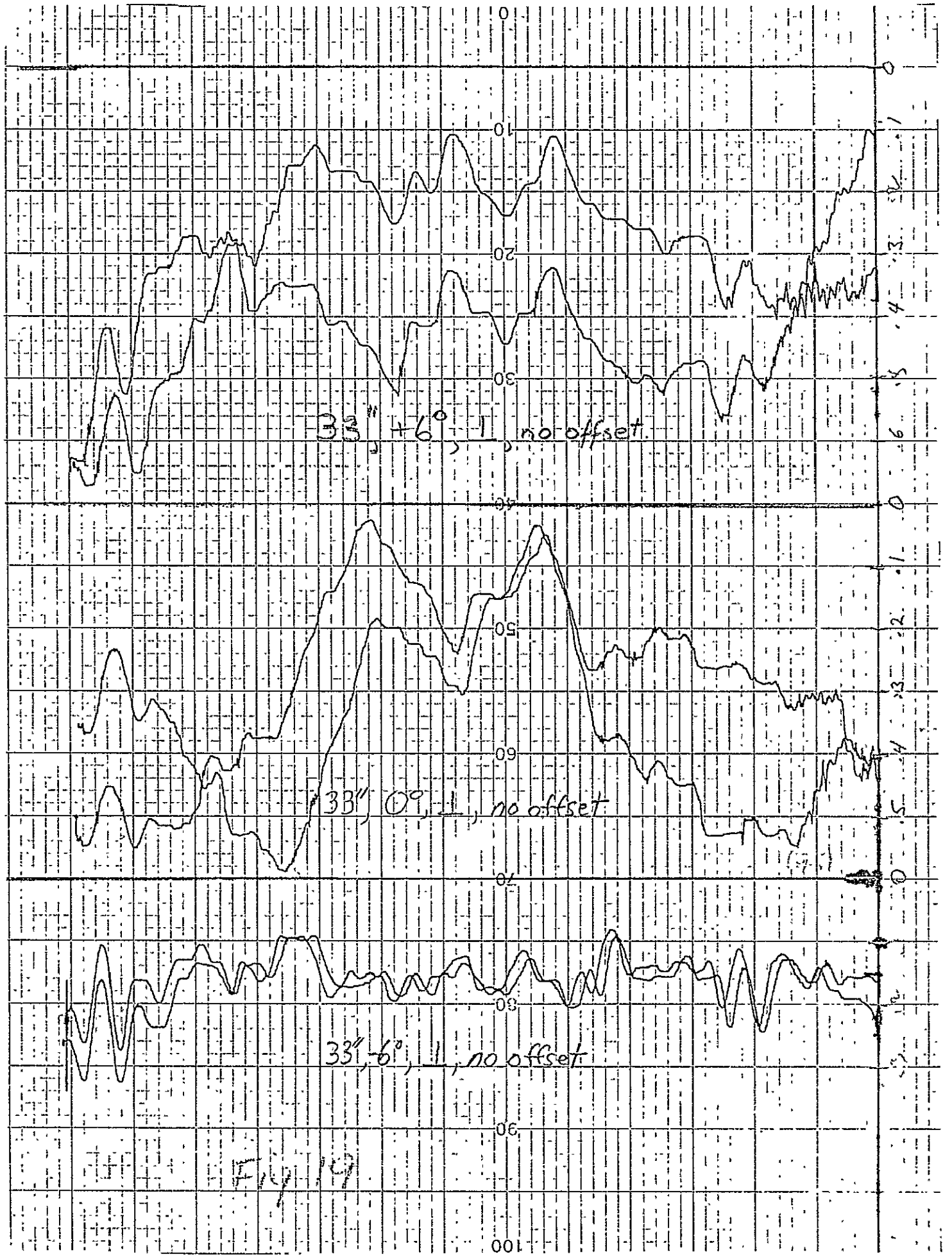
0
10
20
30
33", +6°, ⊥, no offset.
40
50
60
33", 0°, ⊥, no offset
70
80
33", -6°, ⊥, no offset
90
100

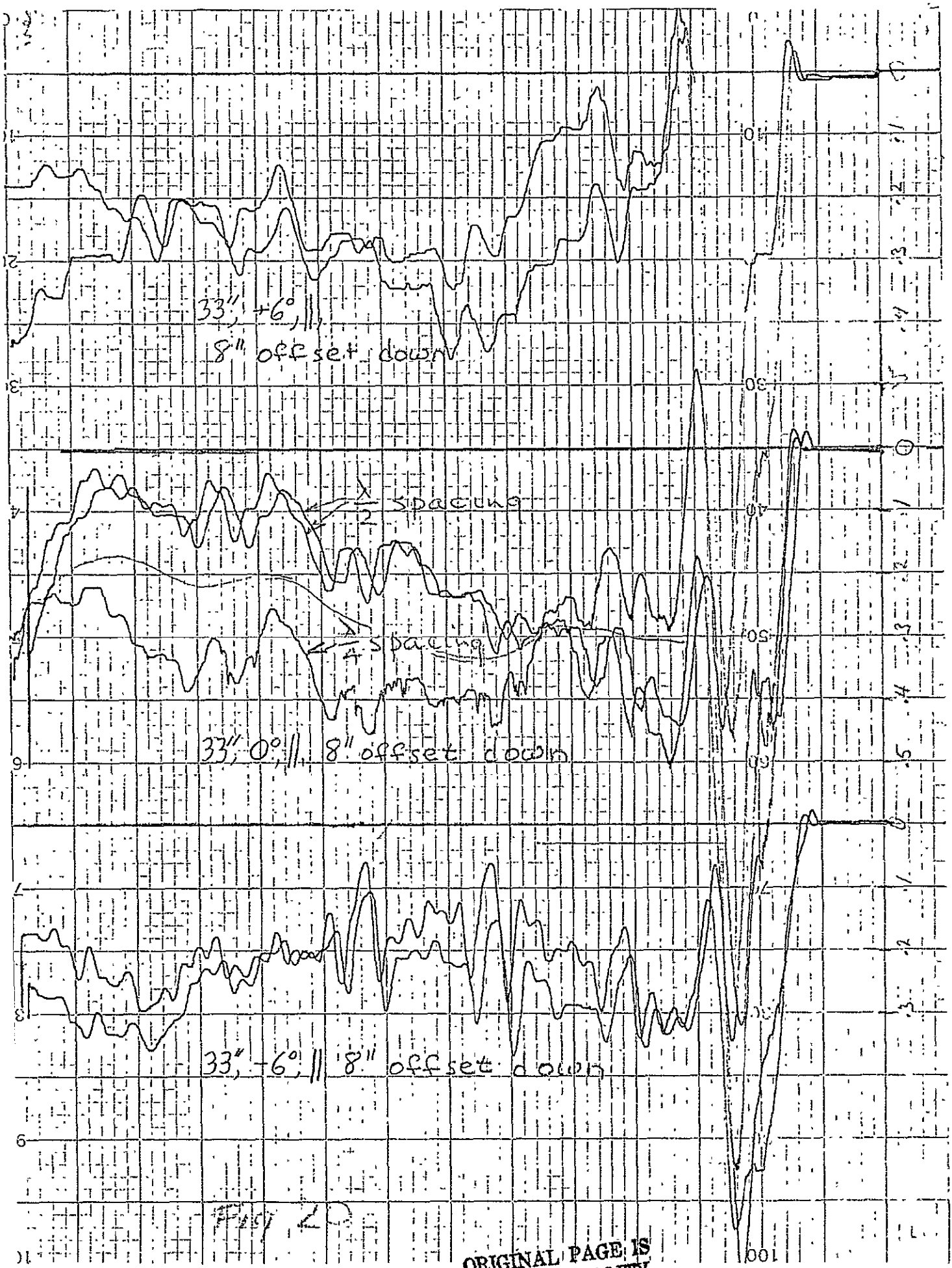

Fig. 2

ORIGINAL PAGE IS
OF POOR QUALITY

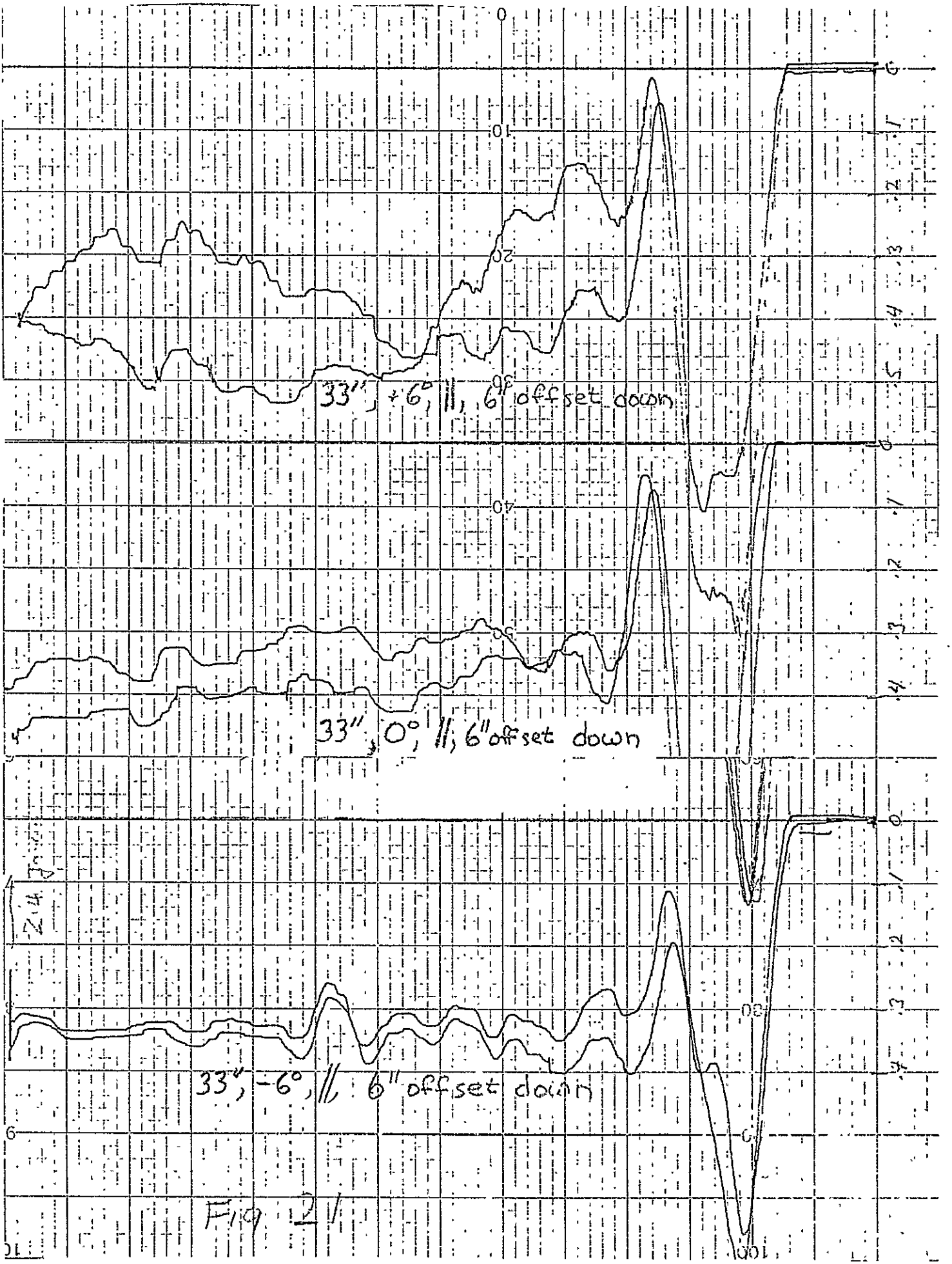

Fig 21

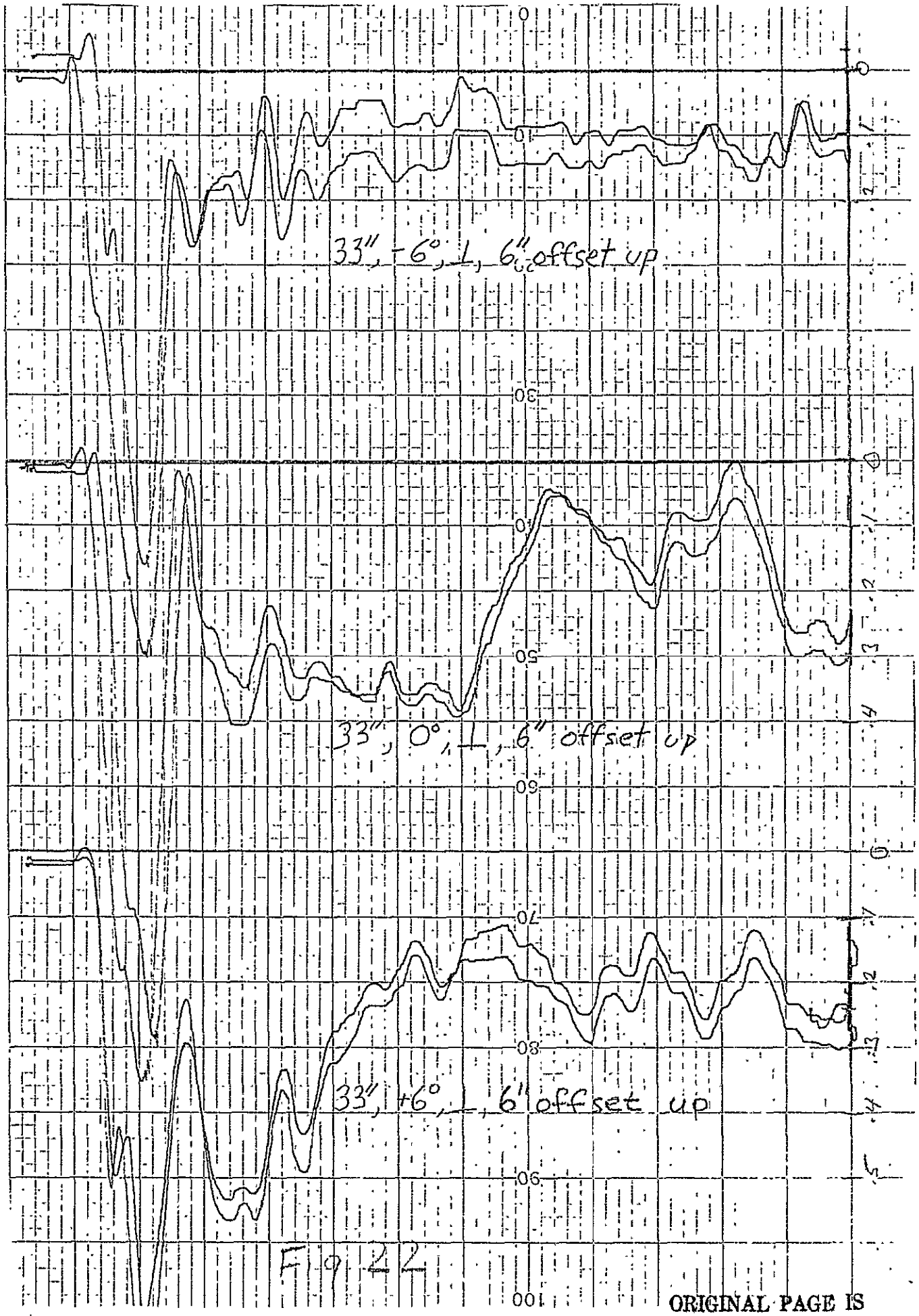

F9.22

ORIGINAL PAGE IS
OF POOR QUALITY

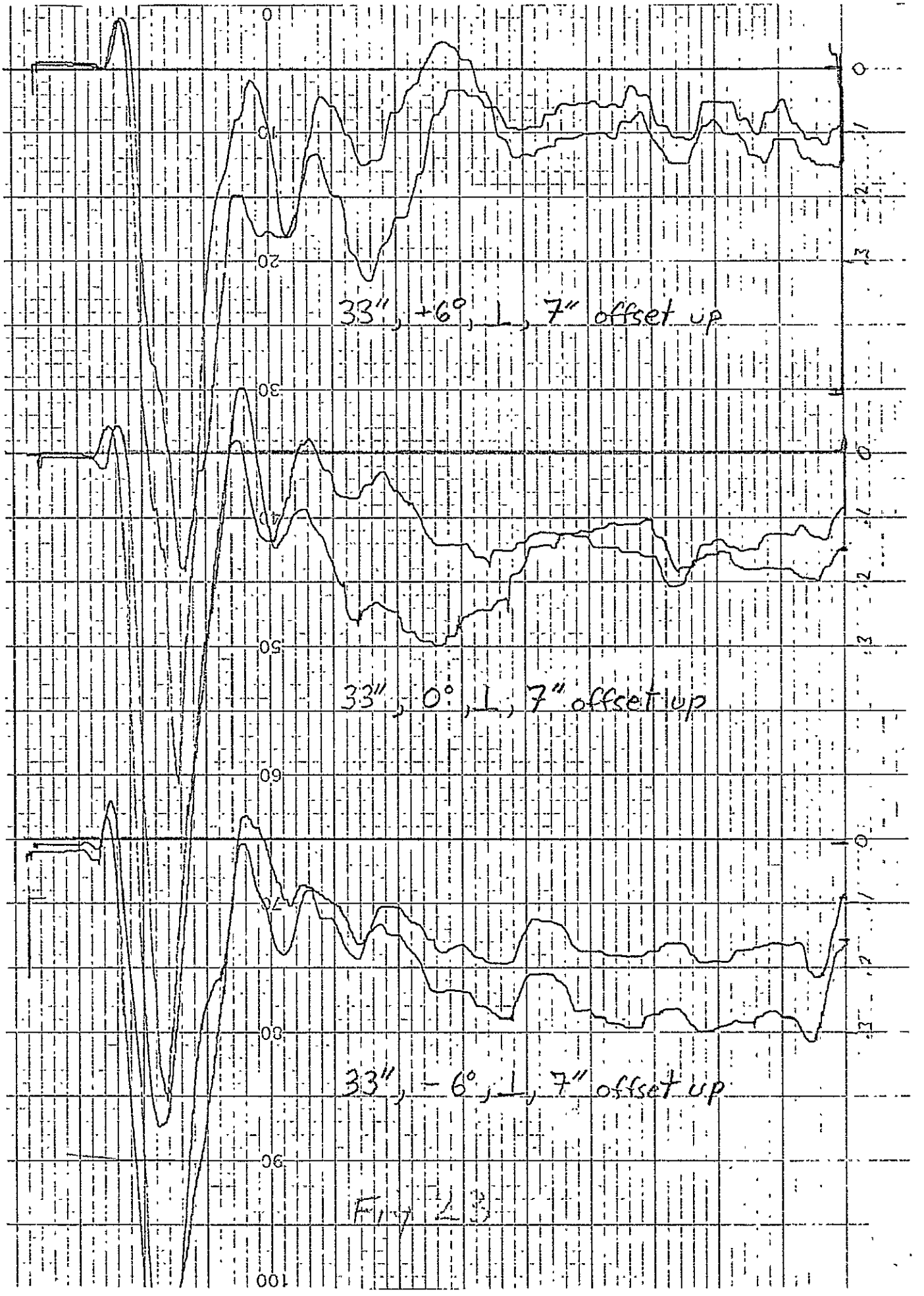

Fig. 7

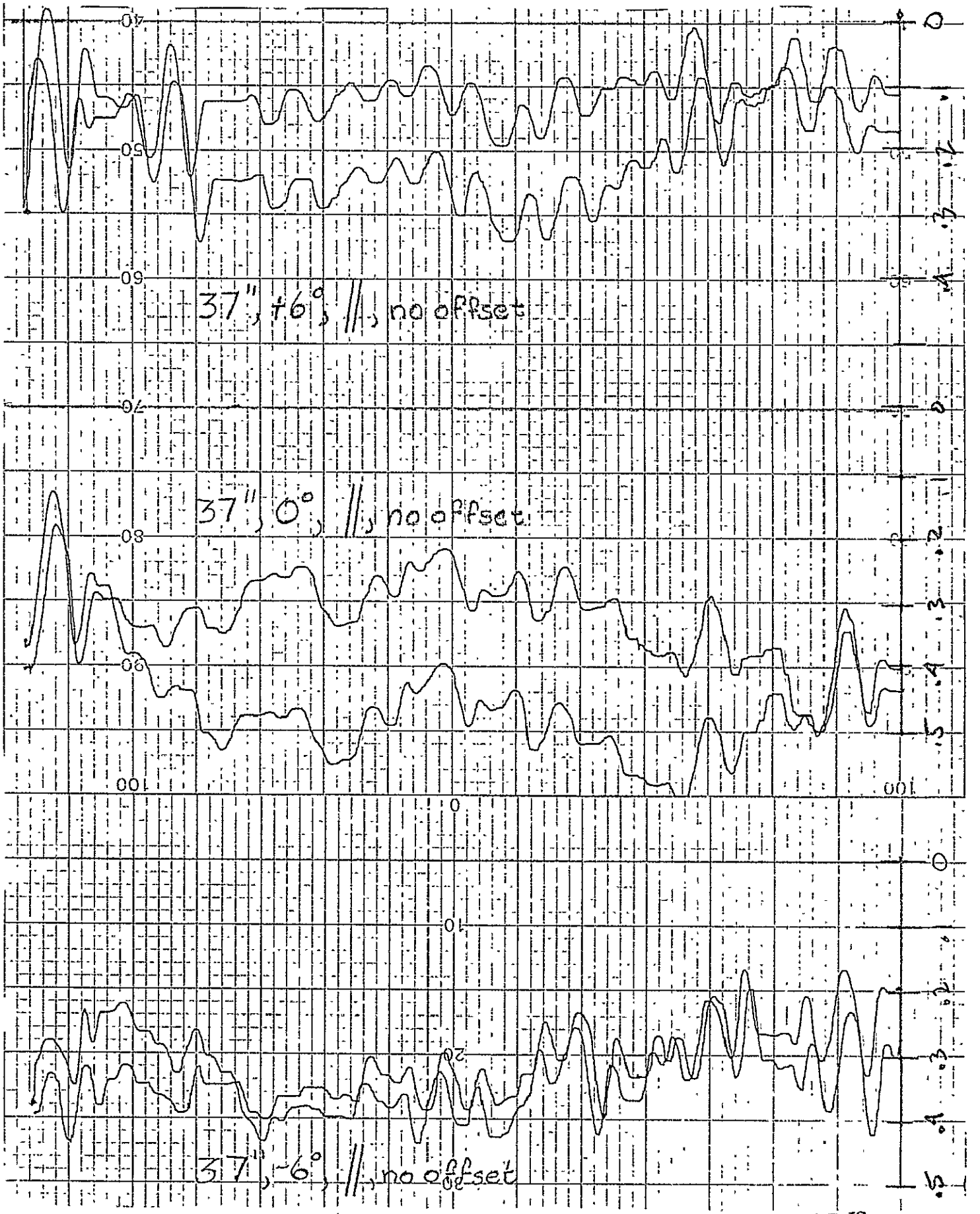

Fig 24

ORIGINAL PAGE IS
OF POOR QUALITY

Fig 25

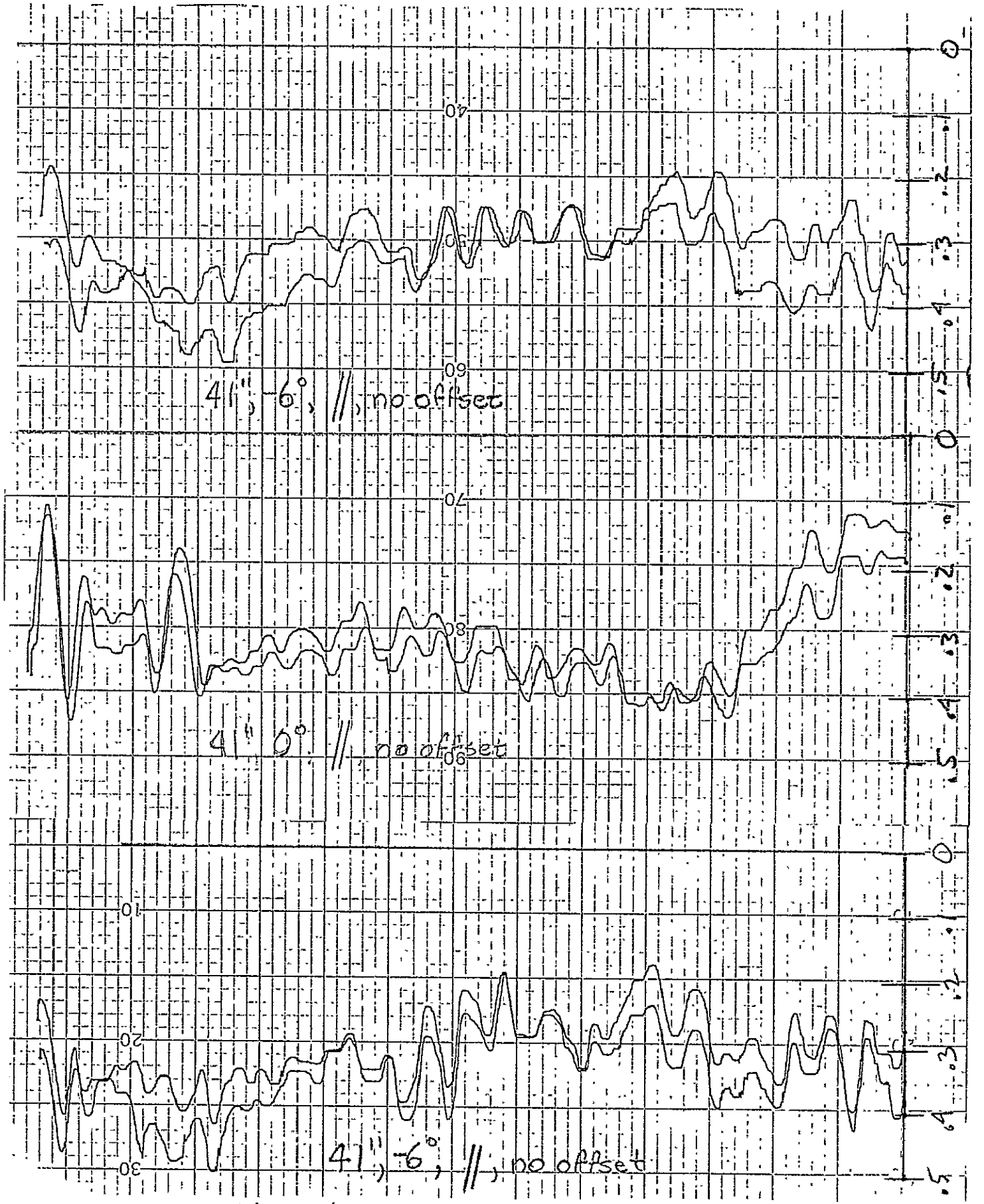

Fig 26

ORIGINAL PAGE IS
OF POOR QUALITY

Fig 27

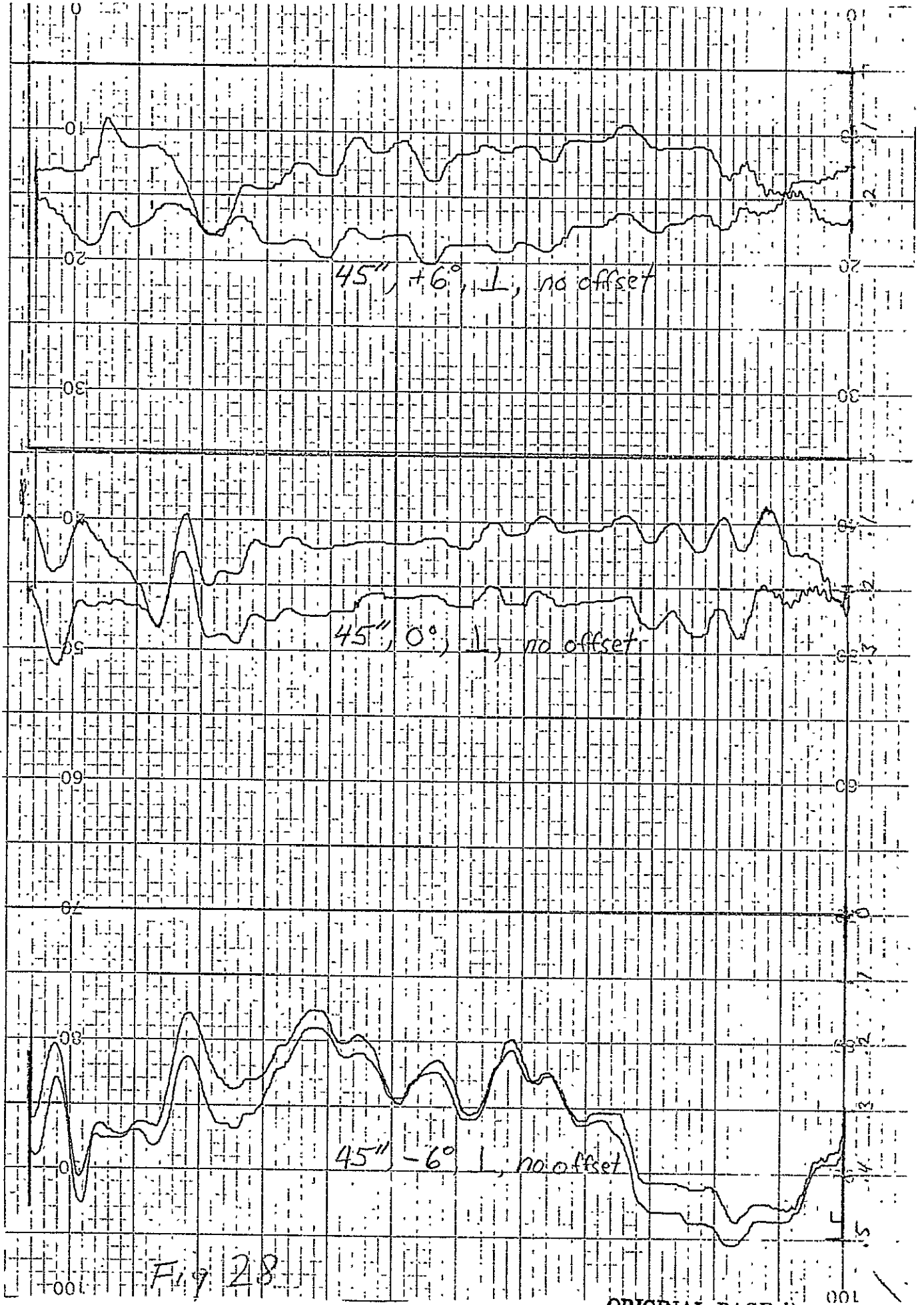

Fig 28

ORIGINAL PAGE IS
OF POOR QUALITY

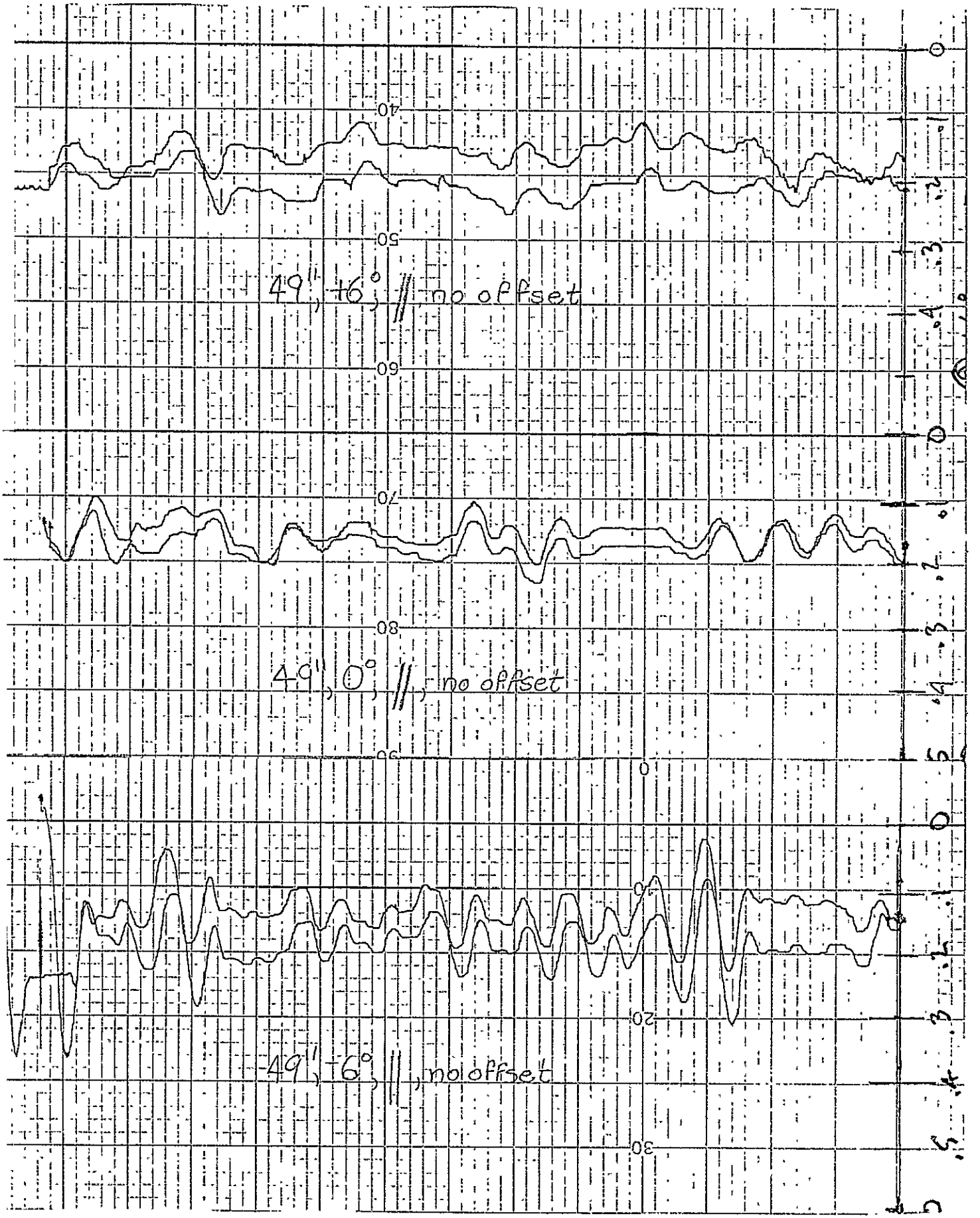
40
50
49', +6°, //, no offset
60
70
80
49', 0°, //, no offset
90
0
20
-49', -6°, //, no offset
30

Fig 29

Fig 30

ORIGINAL PAGE IS
OF POOR QUALITY

Fig 53

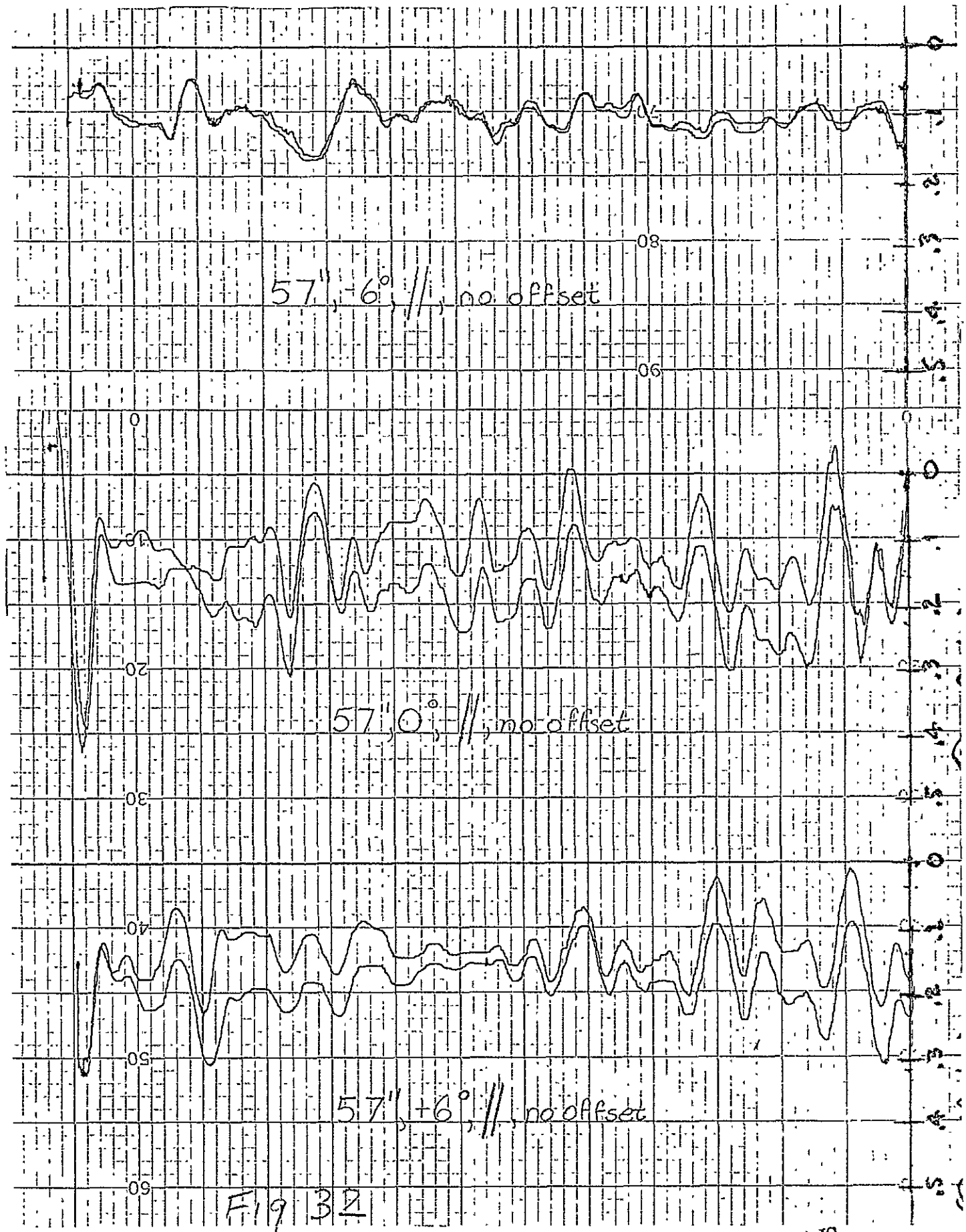

Fig 32

ORIGINAL PAGE IS
OF POOR QUALITY

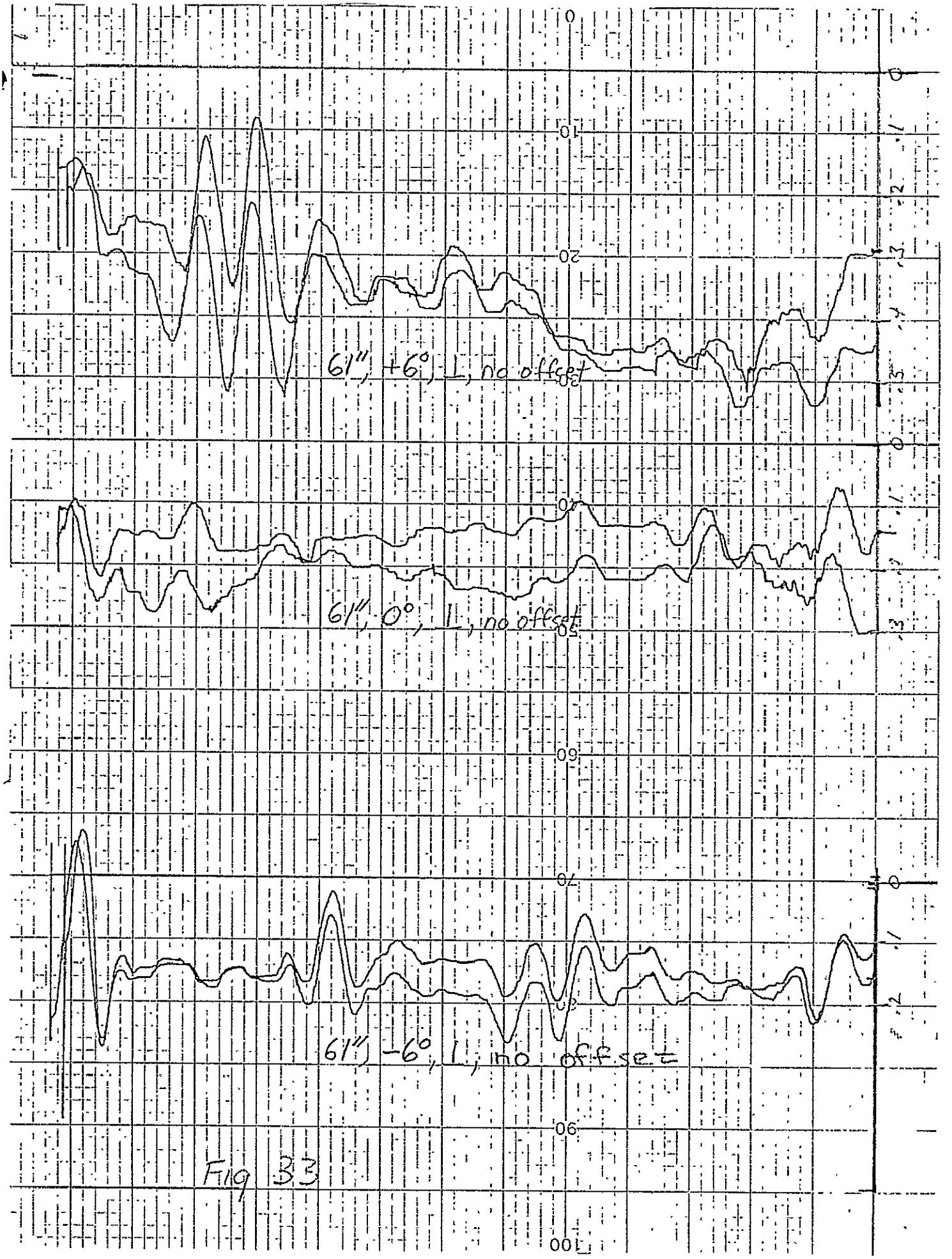

Fig 33

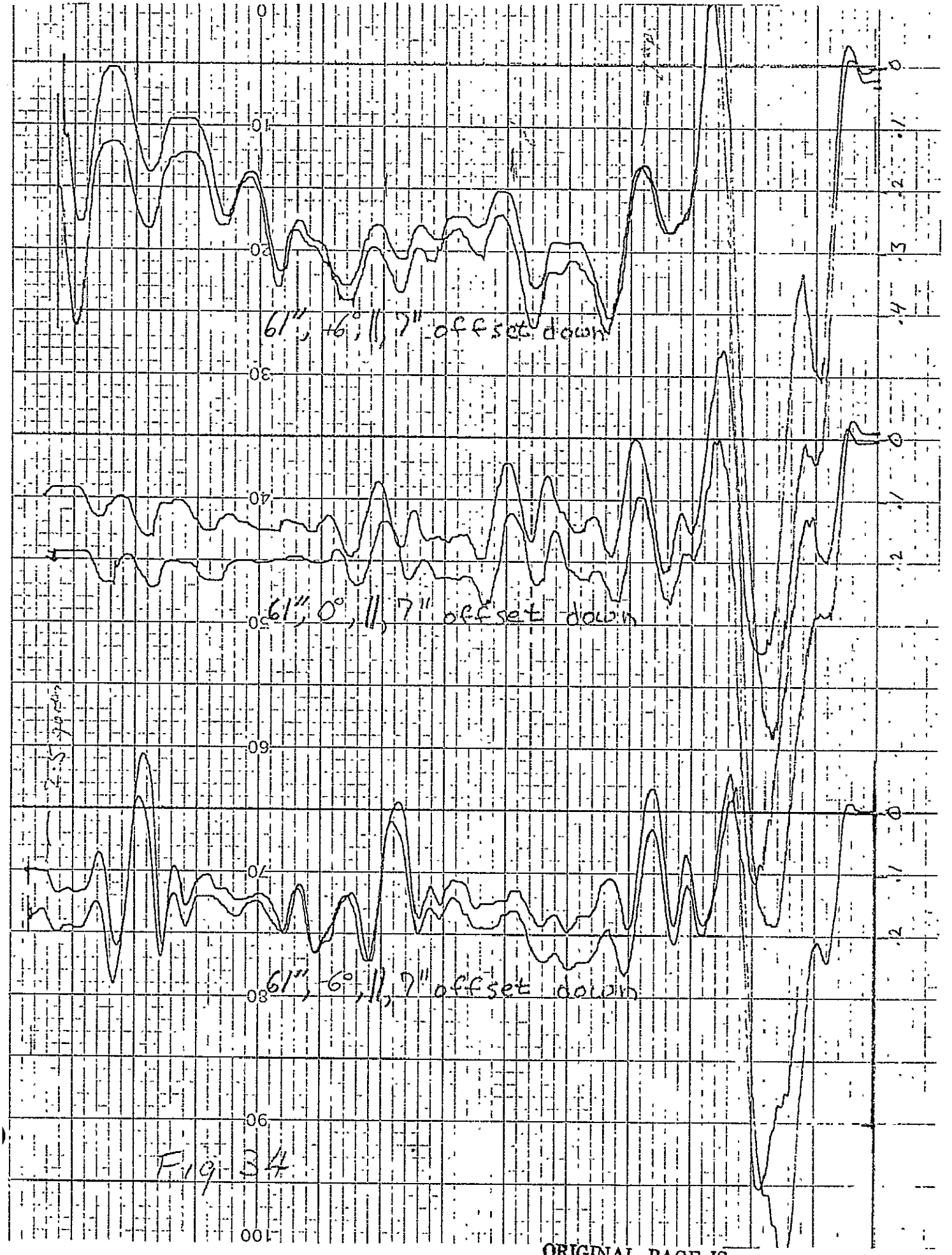

Fig. 34

ORIGINAL PAGE IS
OF POOR QUALITY

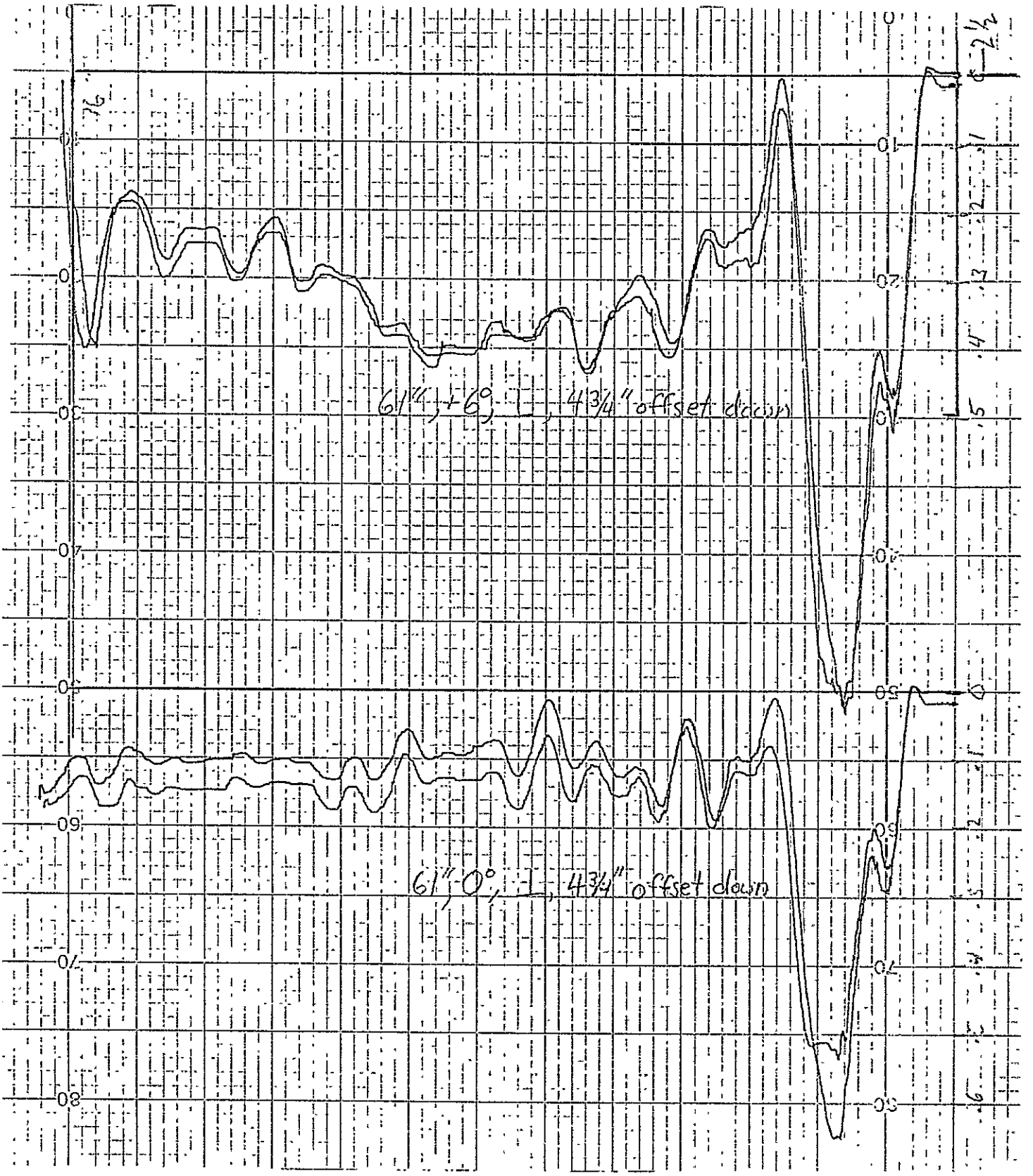

Fig 35

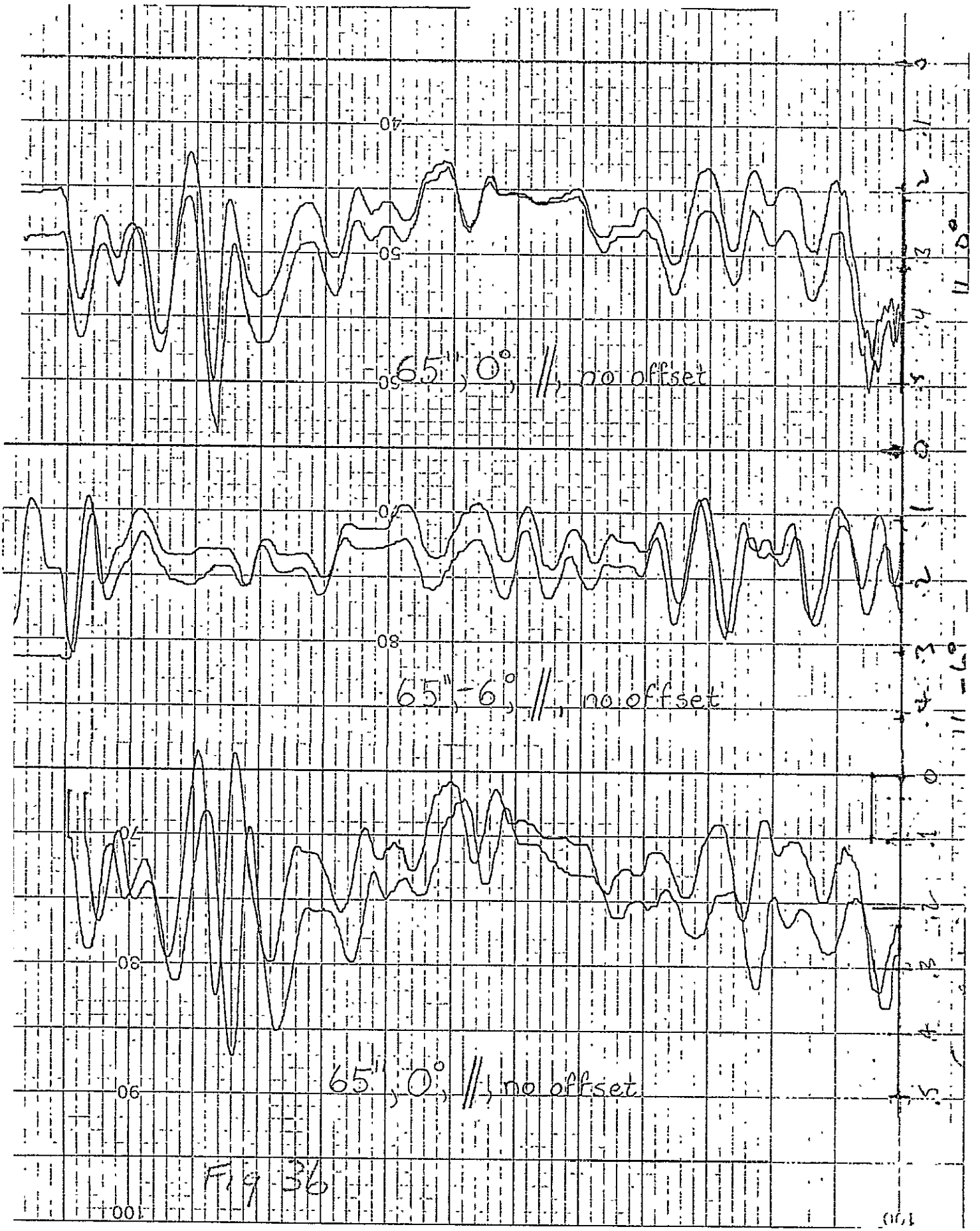

Fig 36

ORIGINAL PAGE IS
OF POOR QUALITY

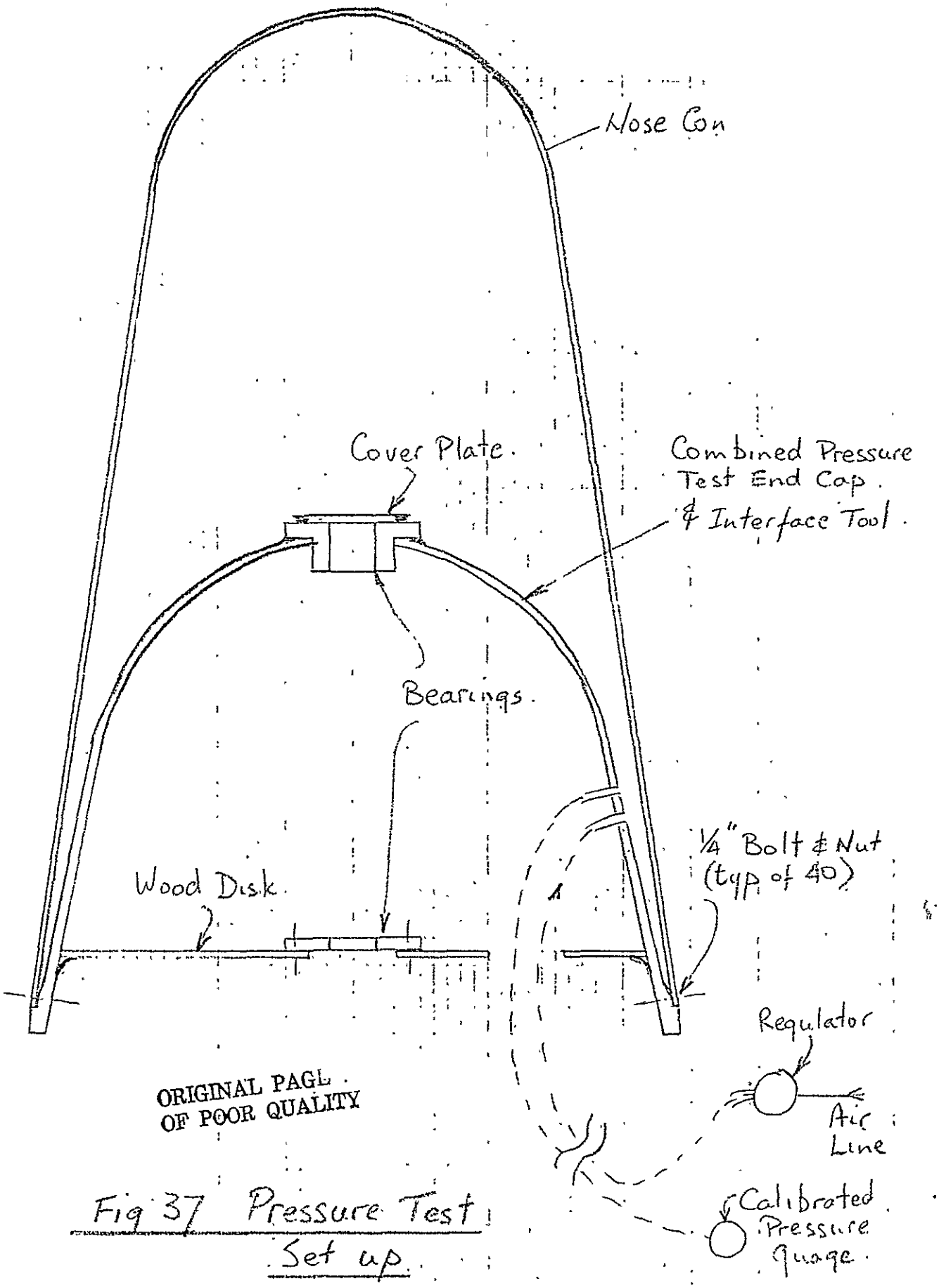

ORIGINAL PAGE
OF POOR QUALITY

Fig 37 Pressure Test Set up

APPENDIX A
Aerodynamic Analysis

WB-57F X-BAND RADOME LOADS ANALYSIS

by

Frederick H. Matteson

Hacking Labs
1043 Di Giulio Avenue
Santa Clara, California

June, 1977

WB-57F X-BAND RADOME LOADS ANALYSIS

SUMMARY

In order to accomodate an X-band radar a radome duplicating the WB-57F nose shape was needed. This report presents the analysis of aerodynamic, inertial and pressurization loads for the flight and ground envelope of conditions necessary to insure that the structure will be safe and suitable. Transverse loads are presented in terms of shears and bending moments.

TABLE OF CONTENTS

I

INTRODUCTION

A.- Background and Objective

The National Aeronautics and Space Administration's Johnson Space Center is conducting Earth resources research using the WB-57F aircraft. Use of an X-band radar is desired, however the standard nose cone and radome is unsuitable. A new radome and nose cone unit was proposed which would retain the external shape of the standard nose cone. Hacking Labs, under Contract Number NAS 9-15189, will construct the new nose cone suitable for the intended radar installation and capable of withstanding the structural loadings and thermal conditions imposed throughout the anticipated ground and flight environment.

The objective of this report is to summarize the design conditions from material supplied by the procuring agency and to furnish design and ultimate loadings in terms of pressures, forces, shears and bending moments. These data will then serve as the basis for design and analysis of the structure.

B.- Government Furnished Data

No special conditions were expected in the operation of the WB-57F aircraft with the X-band radar installed. However the documentation of the design information on the aircraft presented a problem. The original producer of the aircraft, Glenn L. Martin Company, based their design of the B-57 on the English Electric Canberra bomber. Then the B-57 was extensively modified by the General Dynamics Corporation to yield the WB-57F aircraft in 1963. The standard nose cone was one of the modifications carried out by General Dynamics.

The procuring agency furnished data on the design of the aircraft and the standard nose cone and on the operational limitations for the aircraft based on the pilot's handbook. Specifically these included the following:

1. Pages 6-8 and 6-9 of Technical Order 1B-57(W)F-1 giving indicated airspeed and Mach number limitations (red line) versus altitude plus information on flutter and handling qualities at high speeds and altitudes.

2. Page 4-5 from T.O. 1B-57(W)F-1 giving the cabin pressurization schedule.

3. A three-view drawing of the aircraft.

4. Page 3.1.0 of General Dynamics Report FZS-57-005 describing the standard radome structure, attachment and fairing.

5. A listing of ultimate pressurization and inertial loads transcribed from General Dynamics Report FZS-67-005.

6. A page from General Dynamics Report FZS-67-005 giving the above listing and describing the standard radome design, materials, allowable stresses and geometry.

7. Page iii of Report FZS-57-005 giving a list of references.

8. Figures 3.1.1 and 3.1.2 of Report FZS-57-005 showing plots of limit nose radome running airloads and the limit peripheral pressure for 15 degrees sideslip and maximum dynamic pressure.

9. Page A8-3 of T.O. 1B-57(R)F-1-1 giving design maneuver limits versus pressure altitude for the RB-57F aircraft with red outlined values of gross weight of 52,500 lb. and altitude of 60,000 feet.

10. Page 5-8, Figure 5-3 of T.O. 1B-57(W)F-1 giving airspeed limitations versus altitude including some values of true airspeed listed in red.

The material furnished presented a generally consistent basis upon which to establish design and ultimate loading conditions. It did require, however, that certain assumptions be made. These assumptions will be noted in this report.

II

LOADING CONDITIONS

The flight handbook states, "Below 35,000 feet the aircraft is restricted to 190 KIAS, which is the maximum allowable airspeed based on flutter characteristics. Above 35,000 feet the maximum allowable airspeed is 175 KIAS or a Mach Number of 0.80, whichever is less". The airspeed limitations shown on Figure 5-3 of T.O. 1B-57(W)F-1 give a more complex basis of speed limits based on whether outboard tanks are full, gross weight, spoilers open or closed, etc. Normal practice is to design an aircraft to withstand airspeeds in excess of those permitted the pilot. The WB-57F is severely limited by flutter and handling qualities such that it is regarded unlikely that operating limits will be exceeded successfully

ORIGINAL PAGE IS
OF POOR QUALITY

by a large margin. Therefore the limits stated at the start of this paragraph are felt to offer a simple and safe basis upon which to estimate the design airspeeds, which were not expressly stated.

Operating limit speeds for civil aircraft are often established at 90 percent of design values. This basis of determination will be used to arrive at design limit values.

Pilot's Limit Indicated Airspeed	
0 - 35,000 feet altitude	190 knots
35,000 feet and up	175 knots
Pilot's Limit Mach Number	0.80
Design Limit Indicated Airspeed	
0 - 35,000 feet	211.11 knots
35,000 feet and up	194.44 knots
Design Limit Mach Number	0.888

In examining the operational spectrum for conditions which impose the most severe stresses on the structure it is necessary to consider various sources of loading and to determine the extremes for each source. Combinations are then examined to reduce the number of conditions to those resulting in the highest total loads.

The nose cone is subject to loadings resulting from external aerodynamic forces, internal pressurization and from inertial forces. Examination of these sources and the aircraft data furnished can provide guidance in arriving at a set of conditions.

Aerodynamic forces arise from the flow about the nose shape, at zero angle of attack, and from the flow inclination at some angle of attack, sideslip or combination. These forces will, other variables remaining constant, be a maximum where the design indicated airspeed and Mach number are maximum. For a given indicated airspeed the Mach number increases with altitude. For the constant design indicated airspeed of 211.11 knots the highest pressures would be expected to occur at the 35,000 foot maximum altitude for that airspeed. Similarly for the 194.44 knot design indicated airspeed, pressures would be maximized at the 50,000 foot limit. Above 50,000 feet the dynamic pressure, and consequently loads, decreases at a constant limit Mach number.

Pressurization does not commence until 8000 feet altitude where it increases such as to maintain a constant internal pressure until at about 23,000 feet where a constant five

pounds-per-square-inch differential is maintained with increasing altitude. Because of increasing external airloads with altitude, the largest crushing loads at any point on the nose cone will occur at 8000 feet. The critical pressures acting to explode the nose cone will have to be examined at 35,000 and 50,000 feet.

The loads arising from flow inclination are shown in Figure 3.1.1 (Paragraph 1B8 above) to be largest in sideslip (β = 15 degrees). It is assumed that this represents a sudden engine failure condition. The associated inertial loads are expected to be neither large nor well defined. Further, inasmuch as the limit normal load factor for the aircraft is only +2.25, (Figure A8-2, Paragraph 1B9) and the weight of the nose cone is estimated at 200 pounds or less, it is not expected that inertial effects will significantly alter the loadings arising from aerodynamic and pressurization forces and therefore will not be included in establishing the design points on the flight envelope. Separate conditions will be established for inertial loadings.

Summary of Conditions for
Aerodynamic and Pressurization Loads

Condition	Altitude feet	Airspeed (IAS), knots	Mach Number	Pressurization psi.
a	8000	211.11	-	0
b	35,000	211.11	-	5
c	50,000	194.44	-	5
d	50,000	-	.888	5

It is customary to use the ICAO Standard Atmosphere, Reference 1, for airworthiness requirements. The following are taken therefrom:

Altitude, feet	8000	35,000	50,000
Atmospheric pressure, psf.	1571.88	497.96	242.21
Speed of sound, c_s, fps.	1085.74	973.28	968.47
Density ratio, ρ/ρ_o	.78601	.30987	.15223
$(\rho/\rho_o)^{-\frac{1}{2}} = \sigma^{-\frac{1}{2}}$	1.1279	1.7964	2.5630

The true airspeed, TAS, can be calculated from the indicated airspeed, IAS.

ORIGINAL PAGE IS
OF POOR QUALITY

$$TAS = IAS \times \sigma^{-\frac{1}{2}}$$

Mach number, M, is derived from the speed of sound, c_s.

$$M = \frac{TAS}{c_s}$$

Dynamic pressure, q, can be obtained from the Mach number, atmospheric pressure, p, and specific heat ratio, γ. This ratio may be assumed to be equal to 1.40 for atmospheric conditions.

$$q = \frac{\gamma}{2} p M^2$$

The above quantities have been calculated for Conditions a through d and are listed below.

Condition	Altitude, ft.	IAS, fps.	TAS, fps.	M	q
a	8000	356.56	402.16	.370	150.63
b	35,000	356.56	640.52	.658	150.92
c	50,000	328.41	841.71	.869	128.04
d	50,000	335.54	860.00	.888	133.70

Condition c is less severe than d as seen by comparison of both Mach number and dynamic pressure so that it may be eliminated from further consideration. Additional analysis must be made to select those critical from the three remaining.

The ultimate loadings specified by General Dynamics (Paragraph 1B5) do not refer to conditions. Therefore the conditions of flight for the pressurization loads will be assumed to be those listed for design. The inertia loadings are assumed to be incurred on the ground such as during taxiing over an obstacle etc., and do not attend aerodynamic or pressurization loads.

III

AERODYNAMIC LOADS ANALYSIS

A.- Pressures due to Nose Cone Shape

The nose cone at zero inclination of its axis of symmetry to the airstream does not cause transverse forces or moments, but does result in local pressures of a positive or compressive

nature on the forward face and of a negative or suction nature on portions of the sides.

Pressures about semi-infinite bodies in incompressible flow can be calculated by classical hydrodynamic theory, Reference 2. The body most nearly approximating the nose cone is a three-dimensional source in a uniform stream, which is curved with a nose shape almost hemispherical. The equation for the surface in polar coordinates (r, θ) is,

$$\cos\theta + \frac{2\pi U}{m} r^2 \sin^2\theta = 1,$$

where U = free stream velocity
and m = source strength.

The pressures about this source located at the origin are given by the expression,

$$p = \frac{\rho}{2} U^2 \left(\frac{3m^2}{16\pi^2 r^4 U^2} - \frac{m}{2\pi r^2 U} \right),$$

where p = local pressure
and ρ = air mass density.

For scaling purposes the source strength will be assumed equal to 4π times the stream velocity, $m = 4\pi U$. The pressures can be related to the dynamic pressure, $\rho/2\ U^2$ in coefficient form.

$$\text{Pressure coefficient, } P = \frac{p}{\rho/2\ U^2}$$

Making the appropriate substitutions,

$$\cos\theta + \frac{r^2}{2} \sin^2\theta = 1$$

and

$$P = \frac{3}{r^4} - \frac{2}{r^2}.$$

On Figure 1 is shown the shape of the nose cone of the WB-57F and the surface generated by a source. Also shown is the distribution of the pressure coefficient on the source surface. The shape matches the nose cone well up to the location of the source, ten inches behind the nose. Thereafter the source is at first too wide and then too narrow in comparison with the nose cone. A means of producing a shape more closely representing the nose cone and predicting the pressures over it is required.

Von Kármán (Reference 3) used a system of distributed

ORIGINAL PAGE IS
OF POOR QUALITY

doublets to produce bodies of revolution. Similarly a system of sources and sinks can be positioned along the longitudinal axis and, by suitable selection of strengths and locations, can approximate arbitrary bodies. After a number of trials the following arrangement produced a close approximation to the nose cone:

x location, inches	Device	Relative strength
10	Source	1.0
20	Sink	-0.3
30	Source	0.1
65	Source	1.0.

The resulting shape and pressure distribution are shown on Figure 1 as circles. The location of sources are shown by square symbols and the sink as a diamond.

The maximum positive and negative pressures on the nose cone are practically identical to those for the single source. The pressures over the conical portion of the nose cone become positive whereas the downstream pressures for the single source remain negative.

The pressure distribution so derived represents the solution for incompressible flow (M=0). Corrections for compressibility effects can be applied to the incompressible solution to arrive at coefficients for subsonic Mach numbers using the three-dimensional Prandtl-Glauert rule (Reference 4),

$$P_{comp.} = P_{incomp.} \left(\frac{1}{\sqrt{1 - M^2}}\right)^{0.6}$$

The pressures generated by the nose cone shape are summarized for various longitudinal stations in Table I.

B.- Pressures due to Flow Inclination

Transverse forces on the nose cone can arise from oblique flow about it either in the pitch or yaw planes or both. The distribution of such forces would be virtually independent of the direction and can thereby be considered as a single loading condition referenced to the relative wind.

The General Dynamic Figure 3.1.1 provides a chart of running airload on the nose cone at maximum dynamic pressure and at 15 degrees sideslip. It also presents a curve for airload due

to angle of attack. By scaling the curve, the magnitude of the angle of attack was established at 6.5 degrees. No indications of the method used to obtain the loads or the design conditions were given and the peripheral pressures on Figure 3.1.2 contained a sudden discontinuity which was not understood. Attempts to derive the 6.5 degree figure were not wholly successful, however it was apparent that the value would have to be negative, i.e., the relative wind would be from above. The 15 degree sideslip seemed realistic for a single-engine failure mode and was used in combination with the -6.5 degrees angle of attack, which, when added vectorially, results in a 16.35 degrees of flow inclination directed down and from either side at a 23.4 degree angle from the horizontal in a wings level maneuver.

In order to provide a rational method for loads analysis the theory of Reference 5 was used. This theory furnishes both longitudinal and peripheral pressure distributions resulting from inclined flow except at the blunt end of the nose cone, where the limits of flow deflection exceed those of the theory. However the forces and moments produced are predicted and experiments have shown that effects of blunting are generally small except for drag increases for very blunt bodies (Reference 6). The data from Reference 5 indicate that the theory is valid without a compressibility correction if the cross-flow Mach number is small. For a free-stream Mach number of 0.888 and an inclination of 16.35 degrees the cross-flow Mach number, M_c, is,

$$M_c = M \sin\beta = 0.888 \times 0.282 = 0.250.$$

This value is small and no corrections need be made.

The expression for pressure coefficient is based on Reference 5 being,

$$P = (4 \tan\eta \cos\theta)\alpha + (1 - 4 \sin^2\theta)\alpha^2,$$

where $\eta = \tan^{-1}\frac{dR}{dx}$,

θ = azimuth from relative wind,

α = angle of flow inclination,

R = body radius at station x

and x = longitudinal ordinate (axial).

The pressures over the conical portion of the nose cone form a conic so that their values can be tabulated for the values of azimuth angle from the relative wind, θ. Because the dynamic pressure is the same at 8000 and 35,000 feet in these calculations, those results are combined in Table II. Also as two conditions are represented, both right and left sideslip, angles from the aircraft plane of symmetry have two values.

The theory leads to infinite pressure coefficients over the hemispherical nose. In fact the pressures can be expected

ORIGINAL PAGE IS
OF POOR QUALITY

to be very low and must be considered in an analysis even though this part of the structure presents no particular structural problem therefrom. To try to estimate these pressures an artifice will be used. The flow about the inclined hemisphere may, at the extreme, be considered a portion of the flow about a sphere. The flow about the sphere is represented by a three-dimensional doublet (Reference 2). The minimum pressure coefficient produced by the doublet in incompressible flow is -1.25. If the Prandtl-Glauert rule is applied as before the pressure coefficients obtained at 8000, 35,000 and 50,000 feet are -1.306, -1.483 and -1.993 respectively. Multiplying these by the respective dynamic pressures results in pressures of -1.37, -1.56 and -1.85 psi. But because the atmospheric pressure at 50,000 feet is only 1.68 psi., the value obtained at that condition is impossible. Therefore the value of -1.56 psi. found at 35,000 feet will be used as a limiting negative pressure for design purposes.

IV

INERTIA AND PRESSURIZATION LOADS

General Dynamics stated inertia ultimate loads as seven, three and 1.5 g's in the vertical down, horizontal drag and horizontal side directions. Assuming the usual 50 percent factor, design loads then would correspond to 4.67, 2.00 and 1.00 g's. A cursory inspection of aerodynamic and pressurization loadings shows that the horizontal inertia loads are not critical. The vertical loading appears to be of the same order as aerodynamic loads and therefore must be examined.

Design pressurization values were not furnished, however operating pressures were stated to be five pounds per square inch. Ultimate pressures are given as inflight loads plus 8.25 psi. or 11 psi. acting alone. Specification MIL-S-5705 (USAF), dated 14 December, 1954 (Reference 7) was referenced, so was reviewed. In Paragraph 4.2.3.2 the specification reads, "In order to prevent damage to the structure during ground pressurization tests, the design of all parts of the airplane affected by the pressure differential shall be based on a limit differential pressure 33.3 per cent in excess of the highest value specified for the flight operation of the particular airplane. When the parts are investigated for this requirement, only the 133.3 per cent pressure differential shall be applied and all supplementary flight and landing loads shall be ignored". The product of the 33.3 percent pressurization and 50 percent limit-to-ultimate factors results in the ultimate pressurization being twice the operating value. This would, for the 11 psi. value quoted above, result in the operating pressure being 5.5 rather than 5.0 psi. given in the Technical Orders. To be consistent and conser-

vative then, the 5.5 psi. value will be assumed for design purposes.

V

SHEARS AND BENDING MOMENTS

The theory of Reference 5 provides a simple expression for the lift on the nose cone or any portion which also constitutes such a closed body. It is possible to estimate the lift on the hemispherical portion, the entire nose and the difference.

$$L = 2\ q\ S\ \alpha$$

where S = base area

At the tangent point the hemispherical portion has a radius of 14.84 inches. The nose cone has a base radius of 24.00 inches. The corresponding base areas are then 692.07 square inches and 1809.56 square inches. For an angle of attack of 16.34 degrees (0.2854 radians) at 8000 and 35,000 feet altitude with the dynamic pressure of 151 psf., the lift can be calculated,

$$\begin{aligned} L &= 2\ q\ S\ \alpha \\ &= 2 \times 151 \times 1809.56/144 \times 0.2854 \\ &= 1083 \text{ lb.} \end{aligned}$$

At 50,000 feet for the dynamic pressure of 134 psf. the lift is 961 lb.

Using the ratio of areas of the hemisphere to nose cone gives the lift on the hemisphere at 8000 and 35,000 feet,

$$\begin{aligned} L_h &= S_h/S \times L \\ &= 692.07/1809.56 \times 1083 \\ &= 414 \text{ lb.,} \end{aligned}$$

and at 50,000 feet,

$$\begin{aligned} L_h &= 0.3825 \times 961 \\ &= 368 \text{ lb.} \end{aligned}$$

Over the hemispherical nose, which is 12.83 inches in length, the loading will be assumed to be constant. The load per unit length is then,

$$\frac{L_h}{x} = \frac{414}{12.83} = 32.28 \text{ lb./in.}$$

ORIGINAL PAGE .
OF POOR QUALITY

at 8000 and 35,000 feet and,

$$\frac{L_h}{x} = \frac{368}{12.83} = 28.65 \text{ lb./in. at 50,000 feet.}$$

These values are well in excess of those of General Dynamics' Figure 3.1.1 even when allowance is made for the difference in angle of flow inclination.

The conical nature of the isobars over the conical portion of the nose cone leads to a loading proportional to the plan area. At the point of tangency the cone is 29.68 inches wide, 48.00 inches wide at the base and 62.67 inches long. This trapezoid has an area of 2434.10 square inches. The loading ordinates are then equal to the difference between the total nose cone lift and that over the hemispherical portion divided by the width of the trapezoid.

Altitude, feet	Total lift, lb.	L_h, lb.	Difference	Loading front, lb./in.	Loading rear, lb./in.
8000 & 35,000	1083	414	669	8.16	13.19
50,000	961	368	593	7.24	11.70

The loading diagram so developed is shown on Figure 2. The values of loading, shear and bending moment can all be derived at 50,000 feet from the calculations for 8000 and 35,000 feet, given below, simply by means of the multiplication of the values by the ratio of dynamic pressures for the two conditions (134/151 = 0.8874). To obtain the shear the loading is integrated. For the nose where the loading is uniform (x = 0 to 12.83 in.),

$$\text{Loading} = 32.28 \text{ lb./in.}$$

$$\text{Shear} = \int 32.28\, dx = 32.28\, x \Big]_0^x$$

$$\text{Moment} = \int 32.28\, x\, dx = 16.14\, x^2 \Big]_0^x$$

From x = 12.83 to 75.50 this shear is a constant of 414 lb. and the moment generated thereby is 414 (x - 12.83).

For the conical or trapezoidal portion the loading is linear (x = 12.83 to 75.50 in.),

$$\text{Loading} = 8.16 + 0.0803\,(x - 12.83).$$

Substituting y = x - 12.83, then dy = dx,

$$\text{Loading} = 8.16 + 0.0803\, y$$

$$\text{Shear} = 8.16\ y + 0.0402\ y^2$$

$$\text{Moment} = 4.08\ y^2 + 0.0134\ y^3$$

The total shears are shown for the two conditions on Figure 3; the total moments are shown on Figure 4.

Inertia loads are dependent on the weight of the structure, its center-of-gravity location, load factor and direction. To allow flexibility in terms of weight and load factor at the design stage, unit values of 100 lb. for the weight and one "g" for the vertical load factor will be used. Distribution of mass will be assumed to be trapezoidal over the 75.5 inch length with the ends being in the ratio of 15 to 24, which is approximately proportioned to surface area. The mean unit loading is 100 lb. divided by 75.5 inches or 1.324 lb./in., which is the loading at the mean ordinate of 19.5 inches. The end ordinates are 1.019 and 1.630 lb./in.

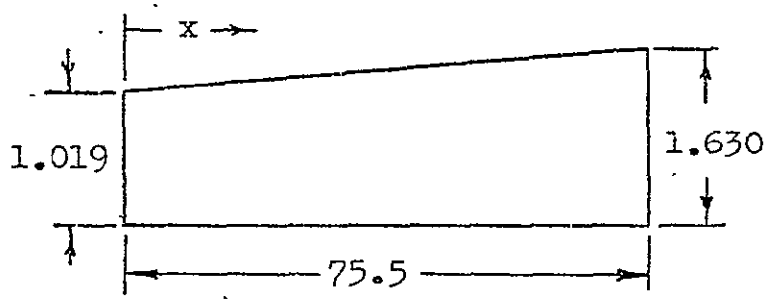

The loading equation is, for x from zero to 75.50,

$$\text{Loading} = 1.019 + 0.008093\ x,$$

$$\text{Shear} = 1.019\ x + 0.004047\ x^2 \text{ and}$$

$$\text{Moment} = 0.5095\ x^2 + 0.001349\ x^3.$$

VI

SUMMARY OF PRESSURES

The maximum positive and negative pressures occur on the spherical portion of the nose cone. The positive maximum is at the stagnation point on the forward face. The maximum negative pressure point is not defined, but should be assumed to act anywhere on the side portions of the hemisphere. The minimum pressures on the conical portion occur approximately 16 inches behind the nose or just aft of the tangent point and at two angular positions each for either right or left sideslip approximately 33 degrees from the aircraft plane of symmetry on top and 13 degrees on the bottom. Maximum positive

ORIGINAL PAGE IS
OF POOR QUALITY

pressures are facing the relative wind. On the conical portion these are maximum at about 47 inches aft of the nose. The design pressures are summarized below.

Altitude, feet	Internal pressure, psi.	Stagnation pressure, psi.	Negative nose pressure, psi.	Positive pressure on cone, psi.	Negative pressure on cone, psi.
0	7.33	0	0	0	0
8000	0	1.096	-1.369	0.375	-.603
35,000	5.50	1.244	-1.554	0.390	-.648
50,000	5.50	1.483	-1.554	0.385	-.688

Thus the largest imploding pressure, taking into account pressurization, is 1.096 psi. at 8000 feet and the largest exploding pressure is 7.054 psi. at either 35,000 or 50,000 feet in flight or 7.33 psi. on the ground.

Table I.- Pressures due to Nose Cone Shape

Distance from nose, x, inches	Incompressible pressure coefficient, $P_{incomp.}$	Pressures, psi.			
		Altitude	8000 feet	35,000 feet	50,000 feet
0	1.0000		1.096	1.244	1.483
5	0.0378		0.042	0.047	0.056
10	-.2611		-.286	-.325	-.387
15	-.2989		-.327	-.372	-.443
20	-.2079		-.228	-.259	-.308
30	-.0685		-.076	-.085	-.101
40	.0575		.063	.072	.085
50	.1043		.115	.130	.154
60	-.0015		-.002	-.002	-.002
75	-.1663		-.183	-.206	-.247

ORIGINAL PAGE IS
OF POOR QUALITY

Table II.- Pressures due to Flow Inclination

Angle from relative wind, θ, deg.	Pressure coefficient	Pressures, psi.			Angle from plane of symmetry, deg.
		Altitude	8000 & 35,000 feet	50,000 feet	
0	0.2483		0.260	0.231	66.57
10	0.2360		0.247	0.219	76.57 or 56.57
20	0.2002		0.210	0.186	86.57 or 46.57
30	0.1446		0.151	0.135	96.57 or 36.57
40	0.0748		0.078	0.069	106.57 or 26.57
50	-.0024		-.003	-.002	116.57 or 16.57
60	-.0794		-.083	-.074	126.57 or 6.57
70	-.1491		-.156	-.139	136.57 or -3.43
80	-.2055		-.215	-.191	146.57 or -13.43
90	-.2443		-.256	-.227	156.57 or -23.43
100	-.2635		-.276	-.245	166.57 or -33.43
110	-.2633		-.276	-.245	176.57 or -43.43
120	-.2464		-.258	-.229	-173.43 " -53.43
130	-.2170		-.228	-.202	-163.43 " -63.43
140	-.1810		-.190	-.169	-153.43 " -73.43
150	-.1446		-.151	-.135	-143.43 " -83.43
160	-.1136		-.119	-.106	-133.43 " -93.43
170	-.0928		-.097	-.086	-123.43 "-103.43
180	-.0855		-.090	-.080	-113.43

CLEARANCE CHARTS

Figure 1.- Shape and Pressure Coefficient Distribution for a Source and the Nose Cone.

ORIGINAL PAGE IS
OF POOR QUALITY

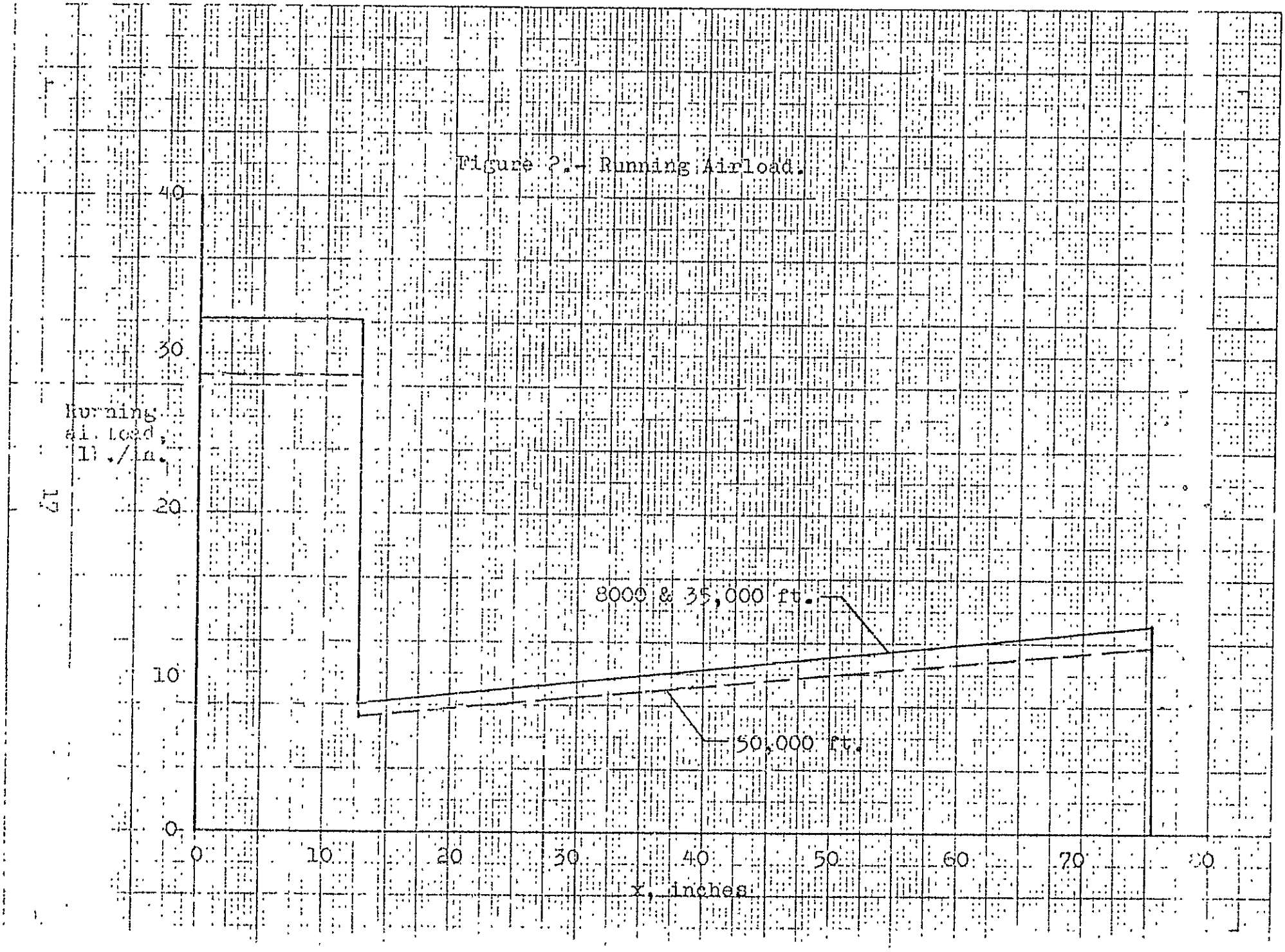

Figure 2.- Running Airload.

Classified Chard

Figure 3.- Airload Shears.

ORIGINAL PAGE IS
OF POOR QUALITY

CLARK-HILL CHARTS

Figure 4.- Airload Moments.

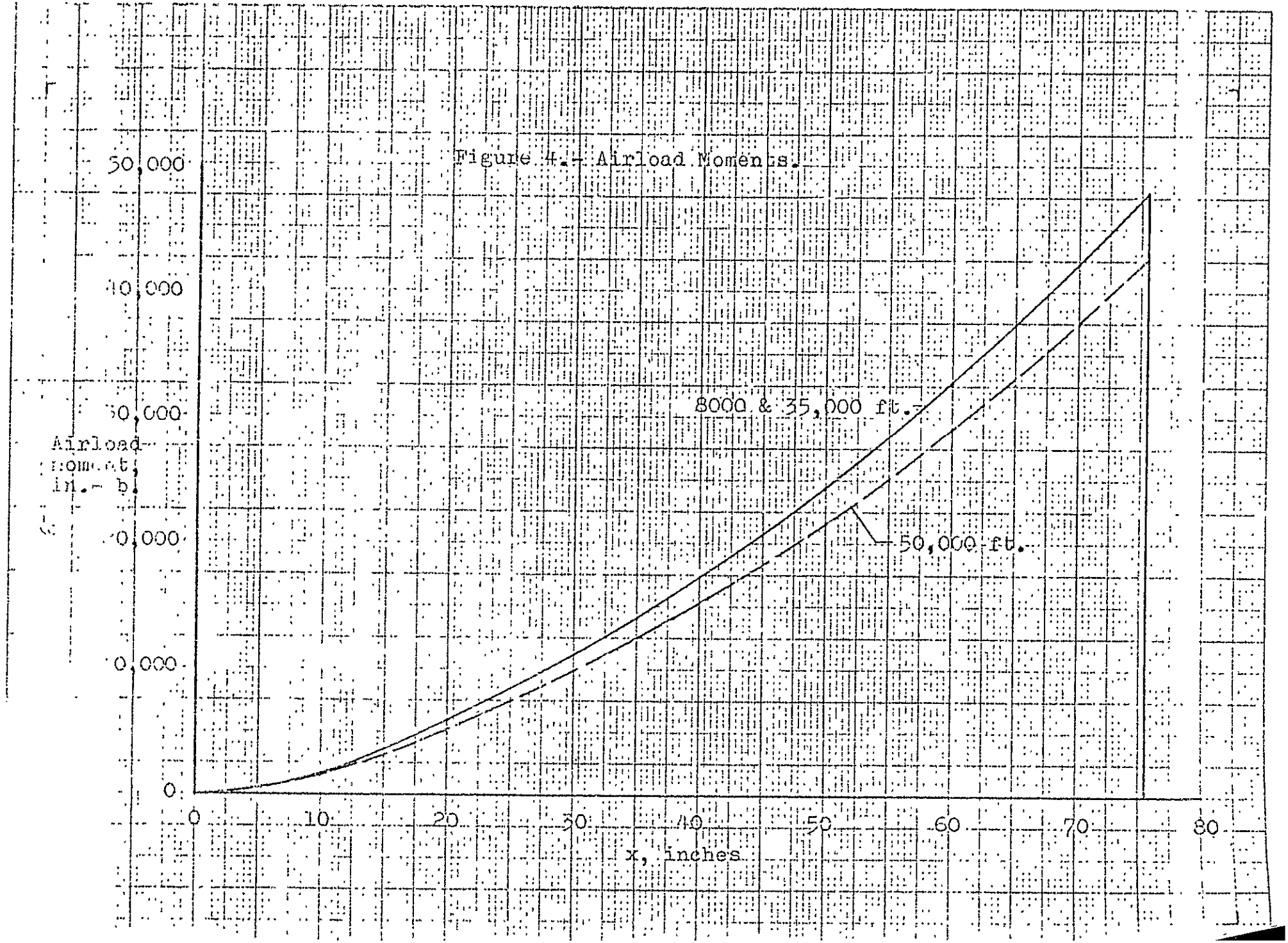

REFERENCES

1. National Advisory Committee for Aeronautics (NACA), Standard Atmosphere - Tables and Data for Altitudes to 65,800 Feet, Report 1235, 1955.

2. Streeter, Victor L., Fluid Dynamics, McGraw-Hill Book Company Inc., New York, 1948.

3. Von Kármán, Theodor, Calculation of Pressure Distribution on Airship Hulls, NACA Technical Memorandum 574, 1927.

4. Hoerner, Sighard F., Fluid-Dynamic Drag, Published by the author, 1965.

5. Allen, H. Julian and Perkins, Edward W., A Study of Effects of Viscosity on Flow over Slender Inclined Bodies of Revolution, Report 1048, 1951.

6. Gapcynski, John P. and Robins, A. Warner, The Effect of Nose Radius and Shape on the Aerodynamic Characteristics of a Fuselage and Wing-Fuselage Combination at Angles of Attack, NACA RM L53I23, 1953.

7. U. S. Air Force, Military Specification Structural Criteria, Piloted Airplanes Fuselage, Booms, Engine Mounts and Nacelles, MIL-S-5705, 14 December, 1954.

ORIGINAL PAGE IS
OF POOR QUALITY

APPENDIX B

STRUCTURAL ANALYSIS
&
DESIGN DETAILS

OF

RADOME - NOSE CONE

PROJECT #22
FOR HACING LABS

BY

N. J. THOMAS - 7/29/77

261 SONDRA WAY

CAMPBELL CALIF. 95008

REPORT #22

GENERAL

AN IN DEPTH REVIEW OF THE "WB-57F X-BAND RADOME LOADS, Je,1977" REPORT BY DR. F. H. MATTESON IN CONJUNCTION WITH THE SPECIFIED MATERIAL FURNISHED FROM THE B-57(W)F HANDBOOK, RESULTED IN THE SELECTION OF THE FOLLOWING LOADING CRITERIA FOR THE NOSE CONE ANALYSIS:

1. 11.0 psi. INTERNAL PRESSURE – ULTIMATE CONDITION
   (SHELL ANALYSIS)
2. INFLIGHT LOADING + 5.5 psi INT. PRESS. – DESIGN CONDITION
   (MECHANICAL FASTENING AT BULKHEAD)
3. INFLIGHT LOADING + ZERO PRESSURE + TEMPT. EFFECTS – DESIGN CONDITION
   (INNER SKIN BUCKLING.)
   - TEMPT. GRADIENT: −80°F, EXTERIOR
     +70°F, INTERIOR

THE REMAINING LIST OF THE LOADING CONDITIONS REVIEWED AND DISCOUNTED ARE:

1. 7G LOADING – ULTIMATE CONDITION: IN VIEW OF NOSE CONE'S RELATIVELY LIGHT WEIGHT (EST. ≤ 100 LBS), THE CRITICAL CALCULATED MOMENT ≤ 29.3 "K LBS LESS THAN THAT OF "INFLIGHT LOADING" CONDITION (48.0 "K) AT THE 8000 FT. AND THE 35000 FT. LEVEL.

ORIGINAL PAGE IS
OF POOR QUALITY

2. INFLIGHT LOADING + 8.25 psi INT. PRESS. ULTIMATE COND.: THIS LOADING CONDITION IS OBVIOUSLY LESS CRITICAL THAN THE DESIGN CONDITION OF "INFLIGHT LOADING + 5.5 psi", AND IT DOES NOT SUPERCEDE THE 11.0 PSI ULTIMATE LOADING CRITERION SINCE THE SHELLS STRUCTURAL INTEGRITY IS INFLUENCED BY LOCALIZED STRESS LEVELS AT THE DISCONTINUITIES WHERE TRANSITION FROM SANDWICH TO SOLID LAMINATE CONSTRUCTION OR FROM LAMINATE TO BULKHEAD OCCUR. SUCH STRESSES ARE PRESSURE DEPENDENT.

3. INFLIGHT IMPLODING LOCALIZED PRESSURES GENERATED DURING FLIGHT. THESE PROVED NOMINAL WHEN LOCAL BUCKLING WAS INVESTIGATED. HERE A CONSERVATIVE APPROACH WAS ADOPTED BASED ON "ROARKS FORMULAS FOR STRESSES AND STRAINS" TABLE XVII, CASE 33, USING A PARABOLIC PRESSURE DISTRIBUTION INSTEAD OF THE UNIFORM PRESSURE SUGGESTED.

ORIGINAL PAGE IS
OF POOR QUALITY

NOSE CONE ELEMENTS & MATERIAL

1. SHELL: SANDWICH CONSTRUCTION USING LAMINATE SKINS AND RIGID FOAM CORE.

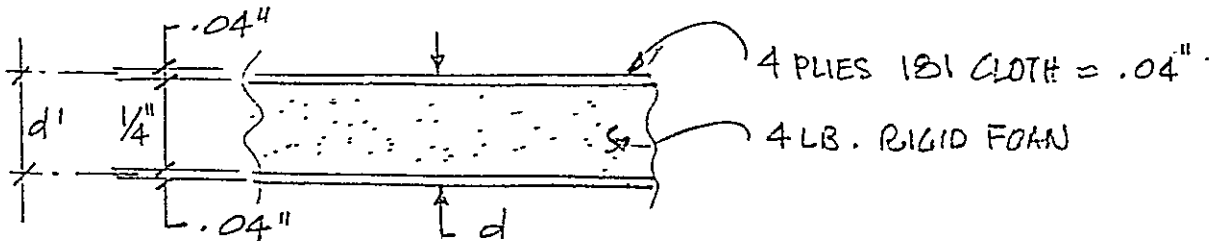

$d = 0.33"$

$d' = 0.29"$

2. DESIGN STRESS LEVELS

σ_b = 16,000 psi DESIGN STRESS ; σ_{ult} = 35 ksi ULT.

σ_{v_c} = 35 psi (CORE) ; τ_{u_c} = 53 psi ULT.

σ_v = 12,000 psi LAMINATE

E = 2.5×10^6 psi MODULUS OF ELASTICITY

$\alpha \leq 6.0 \times 10^{-6}$ in/in PER DEG. F° THERMAL EXPANSION COEF.

3. SHELL MECHANICAL PROPERTIES

$I = 2\left(\frac{d'}{2}\right)^2 \times .04" = 1.68 \times 10^{-3}$ in^4 (MOMENT OF INERTIA)

$S = 2I/d = \frac{2(1.68)10^{-3}}{.33"} = .010$ in^3 (SECTION MODULUS)

$W \leq$ 1.5 LBS/SQ.FT.

ANALYSIS

1. SHELL: (REF. ROARK - FORMULAS FOR STRESS & STRAIN) FOURTH EDITION

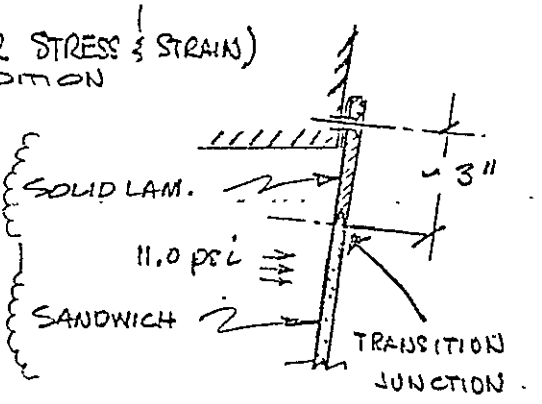

A SIMILTANEOUS SOLUTION OF THE FREE BODY @ THE TRANSITION, WHEN SUPERIMPOSED, RESULTED IN A TRANSVERSE RADIAL SHEAR OF $\leq 13\,^{\#}/_{"}$ AND A MERIDONIAL NOMINAL MOMENT OF $\leq 2\,^{"\#}/_{"}$. THE CRITICAL STRESS HERE IS THE CORE SHEAR (σ_{ν_c})

$$\sigma_{\nu_c} \leq \left(\frac{2}{3}\right) 13.0\,^{\#}/_{"} \left(\frac{1}{.29"}\right) \leq 30\ psi^{\circ}\ (\text{HORIZ. SHEAR}) < 35\ psi^{\circ}\ \text{ALLOW.}$$

& MAX. HOOP STRESS = σ_h

$$\sigma_h = \frac{pR}{t} = \left(\frac{2}{3}\right) 11.0\ psi \frac{24.5"}{.08"} = 2.25^{KSI^{\circ}} < 16.0^{KSI^{\circ}}$$

2. CONE TO BULKHEAD (MECHANICAL ATTACHMEN)

$M_{max} \leq 48.0\,^{"K}$ (35K FT. LEVEL)

$p = 5.5\ psi$ (INTERNAL PRESSURE)

ORIGINAL PAGE IS OF POOR QUALITY

2: (CONT.)

S_c = CONE @ BULKHEAD SECTION MODULUS (SOLID L&M.)

$S_c = \pi R_m^2 d$

$R_m = 24.75" + .33" = 25.08"$ MEAN RADIUS.

$d = .33"$

$S_c = \pi (25.08)^2 (.33") = 650\ in^3$

$\sigma_b = \frac{M}{S_c} = \frac{480^{k}}{650\ in^3} = \pm 74\ psi$

$\sigma_a = \frac{pR}{2d} = \frac{5.5\ psi (24.75)}{2\ (.33")} = +206\ psi$

$\sigma_m = \Sigma = 280\ psi$ (MAX. MERIDONIAL STRESS)

N = No. of SCREWS = 40

$S_p = \frac{2\pi\ 24.75"}{40} = 4"$ SCREW SPACING.

$f_s = \sigma_{max} (d)(S_p) = 280 \times 0.33 \times 4 = 370$ LBS LOAD/SCREW

ASSUME 1/4" COUNTERSUNK SCREWS. $a_s = .027\ \square"$ ROOT AREA

$\tau_s = \frac{f_s}{a_s} = \frac{370}{0.027} = 13.7\ ksi < 14.5\ ksi$ ALLOW.

MAX. SHEAR STRESS

2. (CONT.)

ν_b = BEARING STRESS (LAM.)

$$\nu_b = \frac{f_s}{a_b} \qquad a_b = 0.25" \times .33" = .08\tfrac{1}{4}"$$

$$\nu_b \leq \frac{370^{\#}}{.08\tfrac{1}{4}"} \leq 4.6^{KSI} \quad \text{(Nominal)}$$

3.0 HATCH (DOOR) OPENING

$$T_h \leq \pi R\,(6.0" + 3.0")$$

$$\leq \tfrac{2}{3}(11.0 psi)(\sim 21")(9.0") = 1390^{\#}$$

$$\nu_h \leq \frac{1390^{\#}}{.33" \times 3.0"} \leq \underline{1.4^{KSI}} \text{ Nomial}$$

(Hoop STRESS IN 3" SOLID)

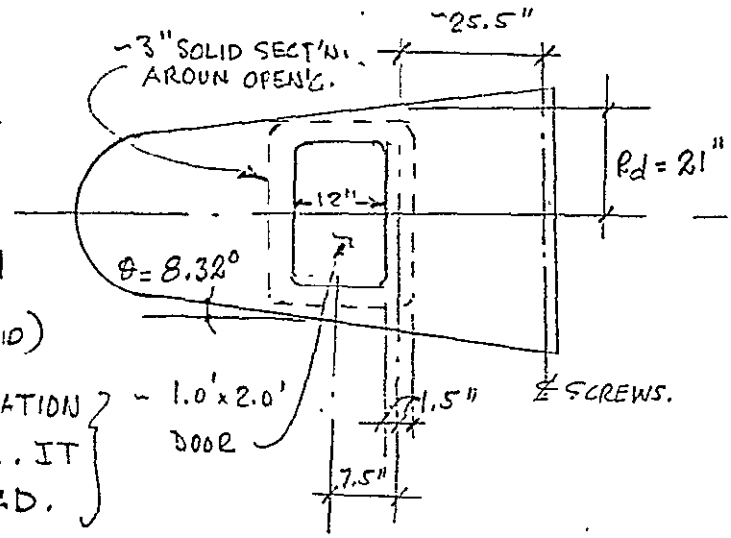

{ BECAUSE OF LOW STRESS, THE LOCATION OF DOOR OPENING IS NOT CRITICAL. IT MAY BE CLOSER TO THE BULKHEAD. }

COMPARE STIFFNESS (6" WITH OF SANDWICH VS 3" SOLID)

$$A_S = 6" \times .08" = 0.48"$$

$$A_{So} = 3 \times .33 = 0.99"$$

$$\frac{A_{So}}{A_S} = \frac{0.99}{0.48} = 2.06$$ RELATIVE STIFFNESS OF SOLID TRIM

AMPLE.

ORIGINAL PAGE IS OF POOR QUALITY

THERMAL EFFECTS

$$\sigma_{h_t} = \sigma_{m_t} = \frac{1}{2}\Delta T \alpha E$$

$$= \frac{1}{2}\left[70^\circ F - (-80^\circ F)\right] 6.0\times10^{-6} \times 2.5\times10^{6} = 1125 \text{ psi}$$

{TENSION - OUTER SKIN
COMP - INNER SKIN}

INFLIGHT MAX. MERIDONIAL STRESS (σ_{b_ϕ})

S_s = SECTION MODULUS (SANDWICH SECTION) ; $R = 24.5"$, $t = .08"$

$$S_s = \pi R^2 t = \pi (24.5)^2 (.08) = 150 \text{ in}^3$$

$$\sigma_{b_s} = \frac{M}{S_s} \leq \frac{48.0^{\text{"k}}}{150} = 320 \text{ psi}$$

$$\sigma_{b_\phi} = \frac{pR}{2t}\sec\theta = \frac{5.5\times24.5}{2(.08")}\sec 8.32^\circ = 850 \text{ psi}$$

σ_{m_t} = 1125 psi

$$\sigma_b = \Sigma = 2295 \sim 2.3^{\text{KSI}} < 16^{\text{KSI}}$$

BUCKLING (HOOP STRESS INNER SKIN - COMP.) ~ 9" FROM BULKHEAD, $R = 24"$

$$\sigma_h' = \frac{E}{4}\left(\frac{t'}{R}\right)^2 = \frac{2.5\times10^6}{4}\left(\frac{.04}{24}\right)^2 = 1735 \text{ psi}$$

$$F.S. = \frac{1735}{1125} = 1.54 > 1.5 \quad (@\ 8000 \text{ FT. LEVEL - ZERO INT. PRESS})$$

NOTE : IN THE ABOVE ANALYSIS THE RESTRAINING EFFECT OF SANDWICH CONSTRUCTION IS IGNORED - CONSERVATIVE

SUMMARY

HAVING EXCLUDED THE LESS CRITICAL LOADING CONDITIONS, THE ANALYSIS BECAME CONFINED TO LOCALIZED STRESS PROBLEMS WHICH ARE PRESSURE SENSITIVE. THUS, THE RELATIVELY SIMPLE & UNIFORM LOADING CONDTIONS SHOWN ON SHEET #1, RULED OUT THE NEED FOR MORE SOPHISTICATED ANALYTICAL TOOLS SUCH AS THE FINITE ELEMENT COMPUTER PROGRAM.

WHEREVER JUDICIAL, AND AS LONG AS THE MINIMUM SAFETY MARGIN OF 0.5 COULD BE ACHIEVED, A CONSERVATIVE ANALYTICAL APPROACH WAS ADOPTED. TO FURTHER ENHANCE THE STRUCTURAL INTEGRITY OF THE NOSE CONE, TWO REP-RESENTATIVE SAMPLES WERE SHEAR TESTED AT HACKING LABS. THE MINIMUM RESULT OBTAINED SHOWED A ~ 50% HIGHER ULTIMATE SHEAR STRESS THAN EXPECTED. THE ANALYSIS, NEVERTHELESS, CONTENDED ITSELF WITH THE MANUFACTURER'S (RIGHT CORE) MINIMUM ULTIMATE STRESS OF 53 PSI OR AN ALLOWABLE DESIGN STRESS OF 35 PSI.

THE THERMAL GRADIENT EFFECTS, TENDING TO MINI-MIZE THE EFFECT OF INTERNAL PRESSURES AT THE CRITICAL TRANSITION POINTS, WERE COMBINED WITH ZERO PRESSURE LOADING CONDITION AND 5.5 PSI CRITERION TO EVALUATE THE BUCKLING SAFETY MARGIN OF THE INNER SKIN AND THE MAX. MERIDIONIAL STRESS LEVEL OF THE OUTER SKIN, RESPECTIVELY.

ORIGINAL PAGE IS
OF POOR QUALITY